Synthesis, Characterization, and Diastereoselectivity of Chloride Substitution Reactions of Cycloruthenated (R)$_C$-(+)-*N*,*N*-Dimethyl-α-(2-naphthyl) Ethylamine

Nizamettin Gül and John H. Nelson*

Department of Chemistry/216, University of Nevada, Reno, Nevada 89557-0020

Received November 2, 1998

The transmetalation reaction of enantiomerically pure (R)$_C$-{HgCl[$C_{10}H_6CH(Me)NMe_2$]}, **1**, with $[(\eta^6\text{-}C_6H_6)RuCl_2]_2$ in CH_3CN at ambient temperature forms a mixture of two diastereomeric ruthenacycles (S_{Ru}, R_C), **2a**, (96%) and (R_{Ru}, R_C), **2a′**, (4%) of the type {(η^6-C_6H_6)Ru[$C_{10}H_6CH(Me)NMe_2$](Cl)} in good chemical and optical yields. The diastereoselectivity of chloride substitution in **2a,a′** by bromide, iodide, azide, cyanate, thiocyanate, nitrite, allylisonitrile, and selected nitrogen and phosphorus donor ligands has been determined by an appropriate combination of ^{1}H, ^{13}C{^{1}H}, and ^{31}P{^{1}H} NMR spectroscopy, UV−visible spectroscopy, circular dichroism, and single-crystal X-ray crystallography. The diastereoselectivity generally increases with increasing steric bulk of the incoming ligand and proceeds with predominant retention of configuration at ruthenium. The ambidentate ligands, cyanate, thiocyanate, and nitrite all bond to ruthenium exclusively through their nitrogen donor atoms.

Introduction

We recently reported[1] the synthesis and characterization of the two enantiomeric ruthenacycles (S_{Ru}, R_C)- and (R_{Ru}, S_C)-{(η^6-C_6H_6)Ru[$C_6H_4CH(Me)NMe_2$](Cl)}. These complexes are among an increasing number of resolved and well-characterized diastereomeric, monoarene ruthenacycles.[2] They are among a smaller number of such complexes that are configurationally rigid in solution under mild conditions. Chloride substitution reactions of these compounds were found[3] to proceed predominantly with retention of configuration at ruthenium. The stereochemistry of these reactions is believed to be under kinetic control and is strongly influenced by intramolecular steric effects. Resolutions of chiral phosphines and arsines with homochiral forms of chloro-bridged palladium(II) complexes containing orthometalated *N*,*N*-dimethyl(α-methylbenzyl) amines and related naphthylamines often proceed better with the naphthylamine complexes.[4] This is thought to result from increased steric interactions in the naphthylamine (TMNA) complexes compared to the benzylamine (TMBA) complexes. Accordingly, we have synthesized and characterized the ruthenacycles (S_{Ru}, R_C)- and (R_{Ru}, R_C)-{(η^6-C_6H_6)Ru[$C_{10}H_6CH(Me)NMe_2$](Cl)} and investigated the stereochemical outcome of the substitution of chloride by a variety of ligands.

Results and Discussion

1. Synthesis and Characterization of 2a,a′. Ruthenacycles **2a,a′** were prepared by the transmetalation reaction of 1 equiv of optically pure (R)$_C$-{HgCl[$C_{10}H_6$-$CH(Me)NMe_2$]}[5] with 0.5 equiv of the dimeric $[(\eta^6\text{-}C_6H_6)RuCl_2]_2$ complex[6a,b] in acetonitrile at ambient temperature (Scheme 1). The ruthenium atom becomes a stereocenter during the course of this reaction, and since the stereochemistry at the benzylic carbon atom remains fixed, only two diastereomers are formed. The chemical yield in this reaction (70.5%) is good, and the product is easily crystallized from a CH_2Cl_2/(hexanes−Et_2O 1:1) mixture.

Each diastereomer shows well-separated resonances, particularly for the H_1, CH, η^6-C_6H_6, and CCH_3 moieties, in the ($CDCl_3$) ^{1}H NMR spectrum, and the diastereomers are stable toward interconversion in solution (vide

(1) Attar, S.; Nelson, J. H.; Fischer, J.; de Cian, A.; Sutter, J.-P.; Pfeffer, M. *Organometallics* **1995**, *14*, 4559.
(2) (a) Dailey, K. K.; Rauchfuss, T. B. *Organometallics* **1997**, *16*, 858. (b) Davies, D. L.; Fawcett, J.; Kvafczyk, R.; Russel, D. R. *J. Organomet. Chem.* **1997**, *545*−*546*, 581. (c) Brunner, H.; Oeschey, R.; Nuber, B. *J. Organomet. Chem.* **1996**, *518*, 47. (d) Brunner, H.; Oeschey, R.; Nuber, B. *Organometallics* **1996**, *15*, 3616. (e) Brunner, H.; Oeschey, R.; Nuber, B. *J. Chem. Soc., Dalton Trans.* **1996**, 1499. (f) Brunner, H.; Oeschey, R.; Nuber, B. *Inorg. Chem.* **1995**, *34*, 3349. (g) Brunner, H.; Oeschey, R.; Nuber, B. *Angew. Chem., Int. Ed. Engl.* **1994**, *33*, 866. (h) Mandal, S. K.; Chakravarty, A. R. *Inorg. Chem.* **1993**, *32*, 3851. (i) Mandal, S. K.; Chakravarty, A. R. *J. Chem. Soc., Dalton Trans.* **1992**, 1627. (j) Mandal, S. K.; Chakravarty, A. R. *J. Organomet. Chem.* **1991**, *417*, C59. (k) Martin, G. C.; Boncella, J. M. *Organometallics* **1989**, *8*, 2863. (l) Consiglio, G.; Morandini, F. *Chem. Rev.* **1987**, *87*, 761. (m) Brunner, H. *Adv. Organomet. Chem.* **1980**, *18*, 151.
(3) Attar, S.; Catalano, V. J.; Nelson, J. H. *Organometallics* **1996**, *15*, 2932.
(4) Wild, S. B. *Coord. Chem. Rev.* **1997**, *166*, 291.
(5) Gül, N.; Nelson, J. H.; *J. Mol. Struct.*, in press.
(6) (a) Bennett, M. A.; Smith, A. K. *J. Chem. Soc., Dalton Trans.* **1974**, 233. (b) Zelonka, R. A.; Baird, M. C. *Can. J. Chem.* **1972**, *50*, 3063.

10.1021/om980895c CCC: $18.00
Publication on Web 01/27/1999

Scheme 1

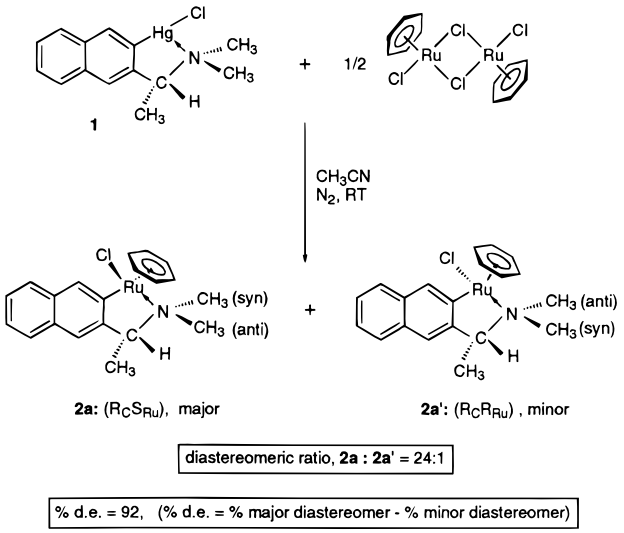

infra). Thus, the stereoselectivity or optical yield can be assessed from the ratio of their integrated intensities. The major-to-minor ratio is 96%:4% (92% de). The ^{1}H NMR spectra obtained on $CDCl_3$, acetone-d_6, and CD_3NO_2 solutions of **2a,a′** are independent of time (days) and temperature (−20 to 50 °C), indicating their configurational stability.[2c,f] Thus, this ratio is under kinetic control.[1]

The solid-state and solution-phase structures of **2a,a′** were elucidated via a combination of X-ray crystallographic and NMR spectroscopic studies. Crystallographic data are presented in Tables 1 and 2 and Figure 1. The geometry around the Ru atom is that of a "three-legged piano stool" in which the η^6-C_6H_6 ligand occupies the "stool" position while the C and N atoms of the naphthylamine ligand and the Cl atom occupy the three "leg" positions. Thus, the Ru atom is in a pseudotetrahedral environment with four different groups attached to it, rendering it a stereocenter. Since the chiral benzylic C atom of the naphthylamino group is not a reaction center, its absolute configuration is unambiguously assigned on the basis of that in the mercury complex starting material: $(R)_C$.[5] The absolute configuration at ruthenium is then assigned assuming the following priority numbers:[7] 1 (η^6-C_6H_6), 2 (Cl atom), 3 (N atom), and 4 (naphthyl C atom): $(S)_{Ru}$. Since the lack of any observable epimerization in this ruthenacycle in solution over a period of several days at ambient temperature, hence its configurational stability, has been established (vide supra), one assumes that the bulk-crystallized sample is a solid mixture of the two diastereomers in a ratio equal to that observed in solution. Thus, we assign the crystal structure (Figure 1) to that of the major species since it follows from the above discussion that the crystals of this species have a higher statistical chance of being isolated from the solution mixture. This argument is supported by the high percent de (92%). All attempts to separate the minor diastereomer by column chromatography and/or fractional crystallization failed; the same solid mixture of diastereomers in the same ratio was always obtained.

(7) (a) Cahn, R. S.; Ingold, C.; Prelog, V. *Angew. Chem., Int. Ed. Engl.* **1966**, *5*, 385. (b) Stanley, K.; Baird, M. C. *J. Am. Chem. Soc.* **1975**, *97*, 6598. (c) Sloan, T. E. *Top. Stereochem.* **1981**, *12*, 1.

The bond lengths and angles of (S_{Ru}, R_C)-[(η^6-C_6H_6)Ru(TMNA)Cl], **2a**, are essentially the same as those of the benzylamine analogue [(η^6-C_6H_6)Ru(TMBA)Cl].[1] Also, for both compounds, in the solid state, the five-membered chelate ring (Figure 1) shows the same puckered envelope conformation with the CCH_3 group in a pseudoequatorial position nearly bisecting the adjacent CNC angle of the $N(CH_3)_2$ moiety and away from the chlorine atom in order to minimize 1,3-diaxial steric interactions.

The solution structures of **2a,a′** were elucidated by ^{1}H and $^{13}C\{^1H\}$ NMR spectroscopic studies (see Experimental Section). Each spectrum exhibits distinct resonances for the arylamine and arene nuclei, which may be assigned to those of the major and minor diastereomers. The observation of two N−CH_3 resonances for each diastereomer indicates that pyramidal inversion at the nitrogen atom is blocked by its coordination to Ru, so that the five-membered chelate ring found in the solid state is also preserved in solution.[5]

The conformation of the chelate ring in solution was probed via ^{1}H difference NOE spectroscopy,[8] which was also of considerable use in the assignment of the ^{1}H chemical shifts. Strong NOEs were observed between the (η^6-C_6H_6) protons, both NCH_3 groups, and the H_1 proton; between the CCH_3 group, H_6, and both NCH_3 groups; between H_1 and H_2; and between H_5 and H_6. Thus, the conformations of this molecule are the same in both the solution and solid states. The puckered chelate ring is rigid and does not change conformation in solution, in contrast to what was observed for the benzylamine analogue.[1] That the most downfield singlet (δ 8.66 ppm) shows a strong NOE to the η^6-C_6H_6 resonance as well as to a doublet of doublets at δ 7.74 ppm allows assignment of these two resonances to H_1 and H_2, respectively. A strong NOE between the narrow doublet at δ 7.18 ppm and a doublet of doublets at δ 7.66 ppm allows assignment of these two resonances to H_6 and H_5, respectively. Assignment of the chemical shifts of H_3 and H_4 was then accomplished by selective proton decoupling and COSY experiments. The ^{13}C chemical shifts were than assigned with the aid of APT and HETCOR experiments.

A CD spectrum of the bulk sample of **2a,a′** (92% de) in the 300−600 nm region is shown in Figure 2. The d−d transitions of the metal chromophore dominate the spectra in this region, with the chiral center in the ligand making little or no contribution to the chiroptical properties.[9] This latter statement is confirmed by the observation that the UV−vis and CD spectra of the mercury starting material are transparent in this region.[5] The morphologies of the CD curves for (S_{Ru}, R_C)-[(η^6-C_6H_6)Ru(TMBA)Cl][1] and (S_{Ru}, R_C)-[(η^6-C_6H_6)Ru(TMNA)Cl] are substantially similar, and in both cases they exhibit a positive Cotton effect in the 450−600 nm region and a negative Cotton effect in the 370−380 nm region. Thus, in both cases there seems to be a clear correlation between the morphology of the CD curve and the absolute configuration at ruthenium.

2. Substitution of Cl by a Halide or Pseudohalide: Synthesis and Characterization of {(η^6-

(8) Stott, K.; Stonehouse, J.; Keeler, J.; Hwang, T.-L.; Shaka, A. J. *J. Am. Chem. Soc.* **1995**, *117*, 4199.

(9) Sokolov, V. I. *Chirality and Optical Activity in Organometallic Compounds*; Gordon and Breach Science Publishers: New York, 1990.

Table 1. Crystallographic Data for 2a-16c′

	2a	3b	4b
emp formula	$C_{20}H_{22}ClNRu$	$C_{20}H_{22}BrNRu$	$C_{20}H_{22}INRu$
fw	412.91	457.37	504.36
cryst syst	monoclinic	orthorhombic	monoclinic
a (Å)	7.0514(6)	10.535(1)	10.741(2)
b (Å)	13.058(2)	11.333(1)	15.258(3)
c (Å)	9.7682(9)	14.712(2)	11.251(2)
α (deg)	90	90	90
β (deg)	103.692(4)	90	98.946(9)
γ (deg)	90	90	90
V (Å^3)	873.9(2)	1756.6(4)	1821.5(6)
Z	2	4	2[c]
space group	$P2_1$	$P2_12_12_1$	$P2_1$
ρ_{calcd} (Mg/m^3)	1.569	1.729	1.839
μ (mm^{-1})	1.049	3.116	2.555
trans max/min	0.9874/0.6352	0.9542/0.2909	0.9678/0.6145
$R(F)^{a,b}$	0.0195	0.0583	0.0398
$R_w(F)^{a,b}$	0.0497	0.1381	0.0934
	5b	**6b**	**7b**
emp formula	$C_{20}H_{22}N_4Ru$	$C_{21}H_{22}N_2ORu$	$C_{21}H_{22}N_2RuS$
fw	419.49	419.48	435.54
cryst syst	orthorhombic	orthorhombic	orthorhombic
a (Å)	10.9370(8)	10.5804(8)	10.1254(4)
b (Å)	11.619(1)	11.398(2)	10.3479(8)
c (Å)	13.8975(9)	14.632(3)	17.986(2)
α (deg)	90	90	90
β (deg)	90	90	90
γ (deg)	90	90	90
V (Å^3)	1766.0(2)	1764.6(4)	1884.5(2)
Z	4	4	4
space group	$P2_12_12_1$	$P2_12_12_1$	$P2_12_12_1$
ρ_{calcd} (Mg/m^3)	1.578	1.579	1.535
μ (mm^{-1})	0.879	0.899	0.948
trans max/min	0.9740/0.8719	0.8554/0.7912	0.9233/0.8662
$R(F)^{a,b}$	0.0315	0.0507	0.0264
$R_w(F)^{a,b}$	0.0524	0.1169	0.0543
	8b	**10c**	**11c**
emp formula	$C_{20}H_{22}N_2O_2Ru$	$C_{25}H_{27}F_6N_2PRu$	$C_{26}H_{29}F_6N_2PRu\cdot H_2O\cdot 0.5CH_2Cl_2$
fw	423.47	601.53	673.01
cryst syst	monoclinic	orthorhombic	monoclinic
a (Å)	10.7211(9)	9.9842(6)	11.121(1)
b (Å)	14.829(1)	13.745(1)	10.815(1)
c (Å)	11.281(1)	17.747(2)	12.348(1)
α (deg)	90	90	90
β (deg)	101.294(7)	90	97.62(1)
γ (deg)	90	90	90
V (Å^3)	1758.8(3)	2435.5(4)	1472.0(3)
Z	2[c]	4	2
space group	$P2_1$	$P2_12_12_1$	$P2_1$
ρ_{calcd} (Mg/m^3)	1.599	1.641	1.518
μ (mm^{-1})	0.907	0.772	0.738
trans max/min	0.9540/0.6410	0.8680/0.8305	0.9503/0.8106
$R(F)^{a,b}$	0.0253	0.0583	0.0647
$R_w(F)^{a,b}$	0.0639	0.1218	0.1727
	12c	**13c**	**14c**
emp formula	$C_{24}H_{24}F_6N_2PRu$	$C_{38}H_{37}F_6NP_2Ru\cdot CHCl_3$	$C_{38}H_{35}F_6NP_2Ru\cdot 0.5$ acetone
fw	586.49	904.06	798.69
cryst syst	orthorhombic	orthorhombic	monoclinic
a (Å)	11.340(1)	11.253(3)	21.628(1)
b (Å)	14.650(1)	17.965(2)	15.0286(9)
c (Å)	14.891(3)	19.184(2)	12.1835(8)
α (deg)	90	90	90
β (deg)	90	90	116.513(7)
γ (deg)	90	90	90
V (Å^3)	2473.9(6)	3878.0(1)	3543.6(4)
Z	4	4	4
space group	$P2_12_12_1$	$P2_12_12_1$	C_2
ρ_{calcd} (Mg/m^3)	1.575	1.548	1.497
μ (mm^{-1})	0.758	0.752	0.595
trans max/min	0.7470/0.7030		0.9145/0.8872
$R(F)^{a,b}$	0.0425	0.0813	0.0363
$R_w(F)^{a,b}$	0.1118	0.1523	0.0978

Table 1 (Continued)

	15c′	16c′
emp formula	$C_{32}H_{35}F_6NP_2Ru$	$C_{26}H_{37}F_6NP_2Ru$
fw	710.62	640.58
cryst syst	monoclinic	monoclinic
a (Å)	11.165(3)	8.651(1)
b (Å)	16.477(6)	16.884(1)
c (Å)	17.407(6)	9.676(1)
α (deg)	90	90
β (deg)	90.42(2)	103.85(1)
γ (deg)	90	90
V (Å^3)	3202.0(2)	1372.2(2)
Z	2[c]	2
space group	$P2_1$	$P2_1$
ρ_{calcd} (Mg/m^3)	1.474	1.550
μ (mm^{-1})	0.647	0.745
trans max/min	0.9882/0.7857	0.9845/0.8769
$R(F)^{a,b}$	0.0397	0.0332
$R_w(F)^{a,b}$	0.0911	0.0788

[a] The data were refined by the method of full-matrix least squares on F^2, with the final R indices having $I > 2\sigma(I)$. [b] $R(F) = \Sigma(|F_o| - |F_c|)^2/\Sigma(|F_o|)$; $R_w(F) = [\Sigma\omega(|F_o| - |F_c|)^2/\Sigma\omega\ |F_c|^2]^{1/2}$; $\omega = 1/\sigma^2(F)^2 = \sigma^2(\text{counts}) + (pI)^2$. [c] Two inequivalent molecules per asymmetric unit.

Table 2. Physical Characteristic of the Crystals of Compounds 2a-16d′

compd	color	habit	size (mm)	solvent(s) used for crystallizn[a]
2a	red	block	0.29 × 0.64 × 0.62	a, b
3b	dark red	hexagonal plate	0.28 × 0.86 × 0.40	c, b
4b	dark red	plate	0.18 × 0.42 × 0.38	a, b
5b	red	block	0.10 × 0.38 × 0.38	a, d
6b	brown	block	0.10 × 0.32 × 0.12	e, d
7b	red	rod	0.20 × 0.35 × 0.30	a, d
8b	yellow	plate	0.20 × 0.82 × 0.80	a, d
10c	golden	rod	0.10 × 0.35 × 0.15	a, d
11c	orange	plate	0.18 × 0.64 × 0.38	a, f
12c	yellow	rod	0.20 × 0.52 × 0.40	a, d
13c	yellow	needle	0.20 × 0.63 × 0.34	c, d
14c	yellow-orange	rod	0.30 × 0.50 × 0.40	g, d
15c′	orange	plate	0.20 × 0.70 × 0.60	a, d
16c′	orange	block	0.31 × 0.42 × 0.36	a, d

[a] Key to solvents used for crystallization: (a) CH_2Cl_2; (b) hexane; (c) $CHCl_3$; (d) Et_2O/hexane (1:1); (e) C_6H_6; (f) Et_2O; (g) acetone. The letters are in order of the addition of solvents.

C_6H_6)Ru[$C_{10}H_6$CH(Me)NMe_2](X)} (X = Br, I, N_3, NO_2, NCS, NCO). The mixture of the chloro complexes (**2a,a′**, 24:1 mixture, 92% de) readily undergoes clean metathesis reactions with an excess of the appropriate sodium salt or a stoichiometric amount of AgNCO[10] in a CH_2Cl_2/(95%) EtOH (1:20) mixture to form the corresponding bromo (**3b,b′**), iodo (**4b,b′**), azido (**5b**), isocyanato (**6b**), isothiocyanato (**7b**), and nitro (**8b**) analogues (Scheme 2) with high chemical and optical yields. These reactions are highly stereoselective, as evidenced by the high ratios of the two diastereomers, **3b:3b′** = 29:1 (93.3% de), **4b:4b′** = 38:1 (94.9% de). For the other four compounds in this series, only one diastereomer could be detected in solution by ^{1}H NMR spectroscopy at 500 MHz. The ^{1}H and ^{13}C{^{1}H} NMR spectra of these compounds are essentially the same as those of the chloro analogues. The azido and isocyanato complexes react slowly with adventitious HCl present in old $CDCl_3$ to form the chloro complex. In both cases the amount of conversion was only a few percent over a period of several days, and only the resonances for **2a** were detected by ^{1}H NMR spectroscopy at 500 MHz. Both complexes are stable in acetone-d_6 solution for several days.

The signs and morphologies of the CD spectra of this series of complexes are very similar (Figures 2 and 3), suggesting that the absolute configurations of the major species in solution are the same.[2f−i,m,11] The absolute configuration at the Ru center of the major diastereomer of the chloro complex has been established as S_{Ru}. Since these diastereomers are configurationally stable and the chirality at the benzylic carbon atom remains R_C during the course of these substitution reactions, we assign to all of these complexes the (S_{Ru}, R_C) and (R_{Ru}, R_C) absolute configurations for the major and minor diastereomers, respectively. The assignments of Ru absolute configuration are opposite to their *formal* designations of R_{Ru} and S_{Ru}, respectively, for two of these complexes (vide infra). These results are similar to those reported[12] for the halide exchange reactions of [(η^5-$C_5H_4R^*$)Ru(CO)(Ph_3P)(X)] (R^* = menthyl, neomenthyl; X = Cl, Br, I).

The above conclusions on the ruthenium absolute configurations for this series of halide and pseudohalide derivatives (and hence the stereochemistry of the reactions leading to their formation) were confirmed by the crystal structures of **3b**−**8b**, the major diastereomers (Figures 4−9). The structures all consist of isolated

(10) Forster, D.; Goodgame, D. M. L. *J. Chem. Soc.* **1965**, 1286.

(11) (a) Wojcicki, A. *Adv. Organomet. Chem.* **1973**, *11*, 87. (b) *Ibid.* **1974**, *12*, 31. (c) Flood, T. C.; Miles, D. L. *J. Am. Chem. Soc.* **1973**, *95*, 6460. (d) Flood, T. C.; Di Santi, F. J.; Miles, D. L. *Inorg. Chem.* **1976**, *15*, 1910. (e) Miles, S. L.; Miles, D. L.; Bau, R.; Flood, T. C. *J. Am. Chem. Soc.* **1978**, *100*, 7278. (f) Davison, A.; Martinez, N. *J. Organomet. Chem.* **1974**, *74*, C17.

(12) Cesarotti, E.; Chiesa, A.; Ciani, G. F.; Sironi, A.; Vefghi, R.; White, C. *J. Chem. Soc., Dalton Trans.* **1984**, 653.

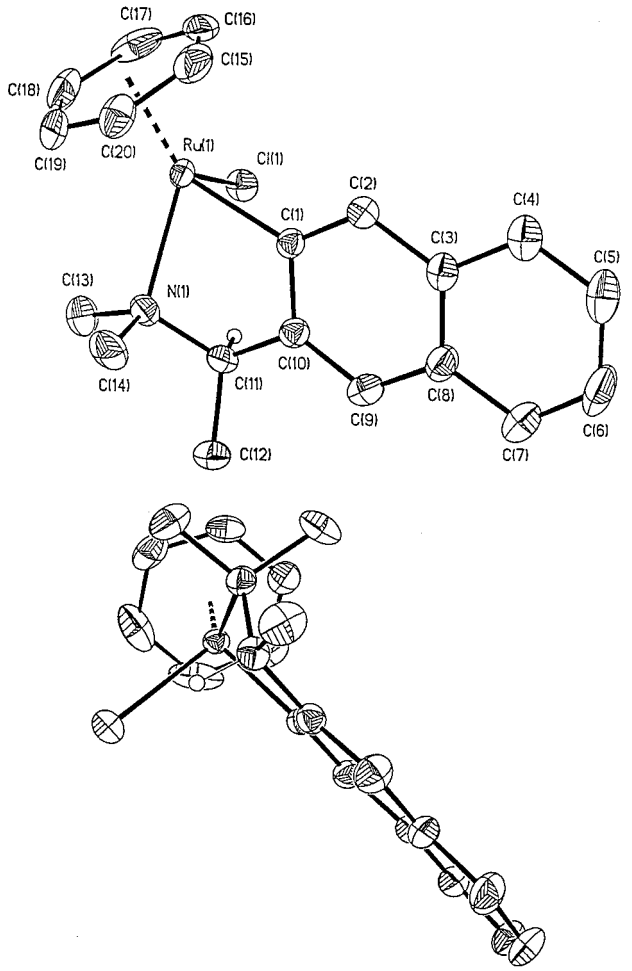

Figure 1. (Top) Structural drawing of **2a**, showing the atom-numbering scheme (40% probability ellipsoids, the hydrogen atom has an arbitrary radius of 0.1 Å). Selected bond lengths (Å) and angles (deg) are Ru(1)−C(1), 2.090(3); Ru(1)−C(arene, av), 2.205(4); Ru(1)−Cl(1), 2.453(1); Ru(1)−N(1), 2.195(3); C(1)−Ru(1)−N(1), 77.0(1); C(1)−Ru(1)−Cl(1) 87.6(1); N(1)−Ru(1)−Cl(1), 89.52(9). (Bottom) Structural drawing of **2a** illustrating the puckered envelope conformation of the five-membered chelate ring.

molecules with no unusual intermolecular contacts. For **4b** and **8b**, the iodo and nitro complexes, respectively, there are two inequivalent molecules in the asymmetric unit with very small differences in their overall structures. The metrical parameters worthy of note are the Ru−C_1 (2.053−2.090 Å; 2.065 Å av), Ru−N_1 (2.116−2.201 Å; 2.173 Å av), and Ru−X (Cl, 2.453(1) Å; Br, 2.573(1) Å; I, 2.747 Å av; N_3, 2.123(5) Å; NCO, 2.097(8) Å; NCS, 2.077(9) Å; NO_2, 2.097 Å av) distances. These distances differ very little among the entire series, and the metrical parameters of the TMBA[1,3] and TMNA analogues are comparable. The ambidentate ligands NCO^-, NCS^-, and NO_2^- all bind to ruthenium through their nitrogen donor atoms, and the Ru−N distances for these three complexes are essentially the same (2.097(8), 2.077(9), and 2.097 Å av, respectively) and are slightly shorter than the Ru−N distance in the N_3^- (2.123(5) Å) complex. The Ru−N distance for the NCS^- complex is similar to those observed[13] for other isothiocyanato complexes of Ru(II) (2.055−2.083 Å). The ^{1}H

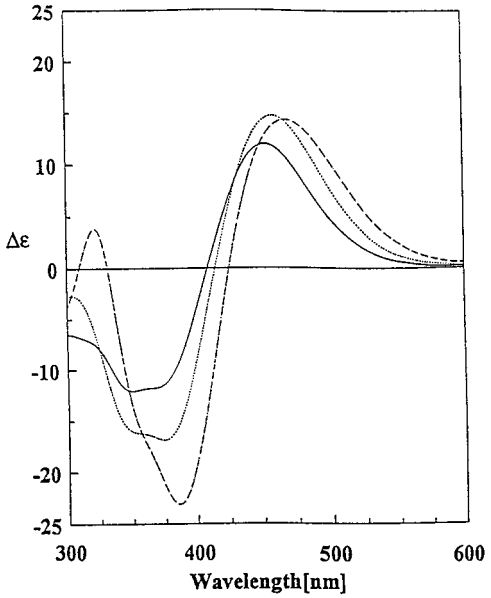

Figure 2. CD spectra of **2a,a′** (— 92% de), **3b,b′** (···93.3% de), and **4b,b′** (- - - 94.9% de) in CH_2Cl_2, 1.8 × 10^{-4} M, 1 cm path length.

Scheme 2[a]

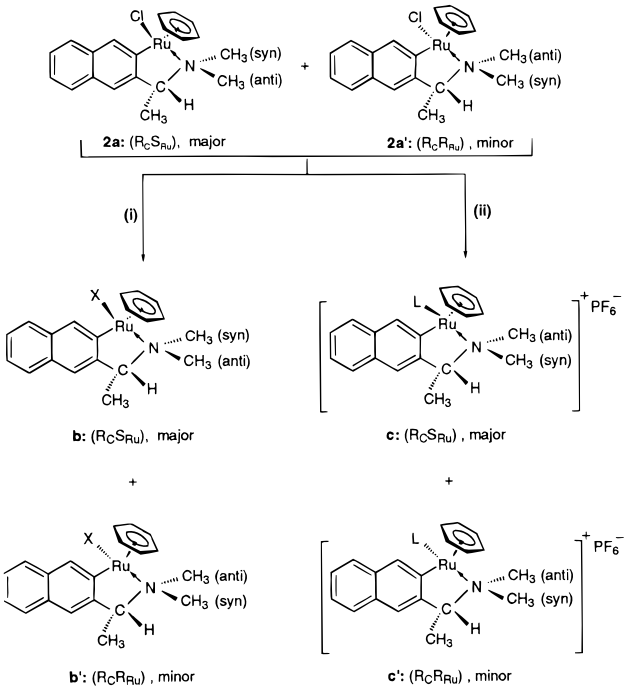

[a] (i) Stirred in EtOH (95%)/CH_2Cl_2 (20:1) mixture with appropriate anion salt at room temperature. (ii) Stirred in EtOH (100%)/CH_2Cl_2 (20:1) mixture with appropriate ligand and $NaPF_6$ at room temperature, under a dry dinitrogen atmosphere.

NMR spectral data for these complexes in solution (only one species is observed in each case), together with the infrared data on the bulk samples in the solid state[14] (see Experimental Section), suggest that these three ambidentate ligands are N-bound in both states. The five-membered chelate ring has the same puckered envelope conformation with the benzylic C−CH_3 group

(13) Homanen, P.; Haukka, M.; Pakkanen, T. A.; Pursiainen, J.; Laitinen, R. H. *Organometallics* **1996**, *15*, 4081.

(14) Nakamoto, K. *Infrared and Raman Spectra of Inorganic and Coordination Compounds*, 5th ed.; Part B: Wiley Interscience: New York, 1997.

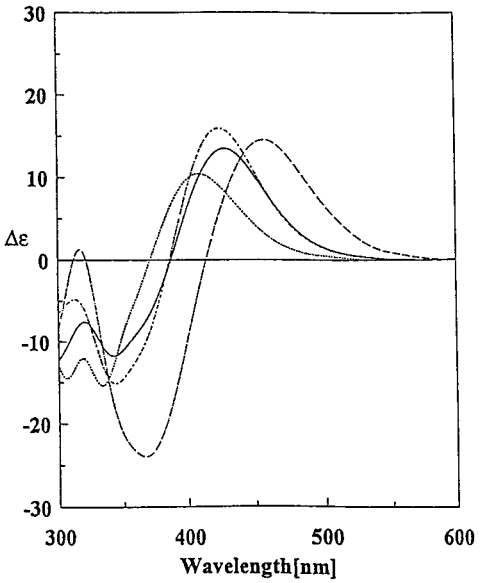

Figure 3. CD spectra of **5b** (- - -), **6b** (—), **7b** (·—·—·), and **8b** (···) in CH_2Cl_2, 1.8×10^{-4} M, 1 cm path length.

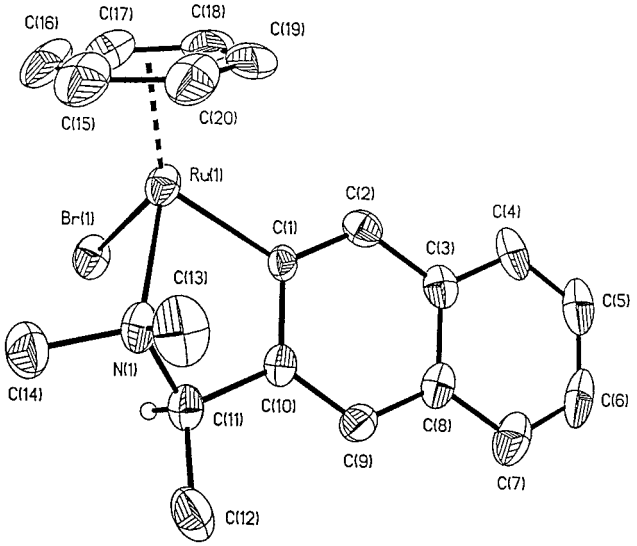

Figure 4. Structural drawing of **3b**, showing the atom-numbering scheme (40% probability ellipsoids, the hydrogen atom has an arbitrary radius of 0.1 Å). Selected bond lengths (Å) and angles (deg) are Ru(1)−C(1), 2.05(1); Ru(1)−C(arene, av), 2.22(1); Ru(1)−Br(1), 2.573(1); Ru(1)−N(1), 2.18(1); C(1)−Ru(1)−N(1), 77.9(4); C(1)−Ru(1)−Br(1) 88.5(3); N(1)−Ru(1)−Br(1), 89.2(2).

pseudoequatorial and nearly in the plane of the aryl ring[4,15] for this entire series of complexes.

The most significant aspect of these structural determinations is the unequivocal assignment of the absolute configuration of the Ru stereocenter. We concluded, on the basis of CD spectroscopy, that the configuration is S_{Ru} for all these complexes. However, on the basis of the assignment of the ligands around the Ru atom in **3b** and **4b**, formally an R_{Ru} configuration is assigned

(15) (a) Van der Schaaf, P. A.; Boersma, J.; Kooijman, H.; Spek, A. L.; Van Koten, G. *Organometallics* **1993**, *12*, 4334. (b) Alcock, N. W.; Hulmes, D. I.; Brown, J. M. *J. Chem. Soc., Chem. Commun.* **1995**, 395. (c) Jiang, Q.; Rüegger, H.; Venanzi, L. M. *J. Organomet. Chem.* **1995**, *488*, 233. The first two citations claim that this conformation is rare, whereas the third claims that it is found approximately 50% of the time for such rings.

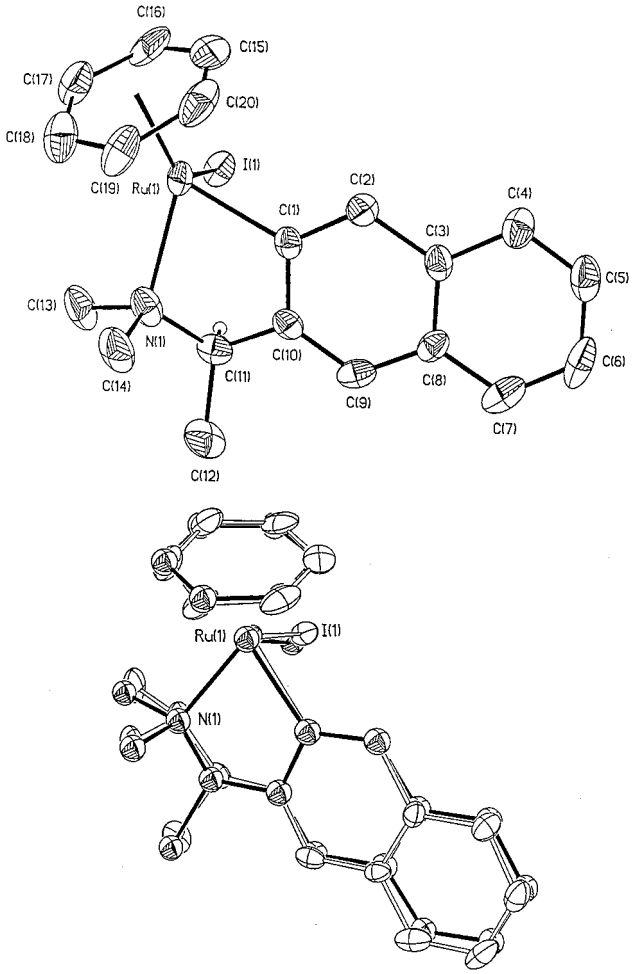

Figure 5. (Top) Structural drawing of **4b**, showing the atom-numbering scheme (40% probability ellipsoids, the hydrogen atom has an arbitrary radius of 0.1 Å). Selected bond lengths (Å) and angles (deg) are Ru(1)−C(1), 2.07(1); Ru(1)−C(arene, av), 2.20(1); Ru(1)−I(1), 2.735(1); Ru(1)−N(1), 2.21(1); C(1)−Ru(1)−N(1), 77.6(4); C(1)−Ru(1)−I(1) 86.4(3); N(1)−Ru(1)−I(1), 90.7(3). (Bottom) Superposition of the two independent molecules of **4b**.

from the crystal structure data. The change in the *formal* designation of configuration merely arises from a change in the position of the halide atom in the ligand priority sequence,[7] where the ligand priority is η^6-C_6H_6 (1) > Cl (2) > N (3) > C (aryl) (4), but I/Br (1) > η^6-C_6H_6 (2) > N (3) > C (aryl) (4). A comparison of the structure of **2a** with those of **3b** through **8b** shows that the absolute stereochemical arrangements of the ligands (atoms) around the Ru centers in these complexes are the same. Since these complexes are configurationally stable in solution for days, these chloride substitution reactions proceed with predominant retention of configuration at ruthenium for the major diastereomer. In the bromide reaction 17% of the minor diastereomer undergoes inversion, in the iodide reaction 36% of the minor diastereomer undergoes inversion, and in the azide, isocyanate, isothiocyanate, and nitrite reactions, at our experimental limits of detection, all of the minor diastereomer undergoes inversion.

3. Substitution of Cl by Nitrogen and a Carbon Donor: Synthesis and Characterization of {(η^6-C_6H_6)Ru[$C_{10}H_6CH(Me)NMe_2$](L)}$^+PF_6^-$.A.L = CH_3CN,

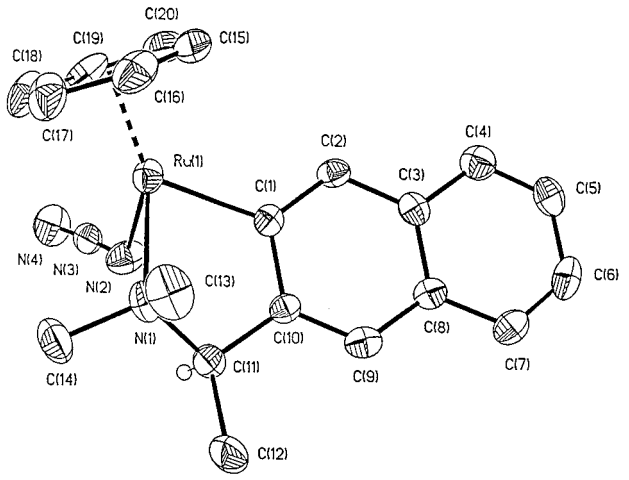

Figure 6. Structural drawing of **5b**, showing the atom-numbering scheme (40% probability ellipsoids, the hydrogen atom has an arbitrary radius of 0.1 Å). Selected bond lengths (Å) and angles (deg) are Ru(1)−C(1), 2.065(4); Ru(1)−C(arene, av), 2.208(6); Ru(1)−N(2), 2.123(5); Ru(1)−N(1), 2.185(4); N(2)−N(3), 1.181(6); N(3)−N(4), 1.161(6); C(1)−Ru(1)−N(1), 78.4(2); C(1)−Ru(1)−N(2), 85.4(2); N(1)−Ru(1)−N(2), 82.3(2); Ru(1)−N(2)−N(3), 124.3(4); N(2)−N(3)−N(4), 176.2(6).

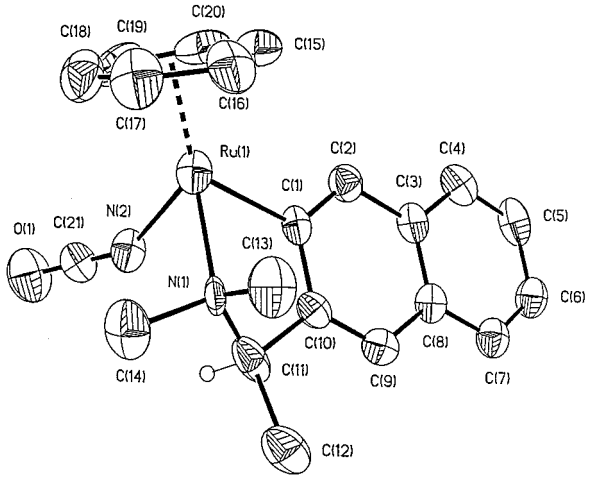

Figure 7. Structural drawing of **6b**, showing the atom-numbering scheme (40% probability ellipsoids, the hydrogen atom has an arbitrary radius of 0.1 Å). Selected bond lengths (Å) and angles (deg) are Ru(1)−C(1), 2.062(8); Ru(1)−C(arene, av), 2.22(1); Ru(1)−N(2), 2.097(8); Ru(1)−N(1), 2.143(7); N(2)−C(21), 1.14(1); C(21)−O(1), 1.19(1); C(1)−Ru(1)−N(1), 76.1(3); C(1)−Ru(1)−N(2), 86.8(2); N(1)−Ru(1)−N(2), 81.9(3); Ru(1)−N(2)−C(21), 153.2(9); N(2)−C(21)−O(1), 178.8(12).

9c,c′. Acetonitrile complexes of the type $\{(\eta^6\text{-}C_6H_6)Ru(TMNA)(CH_3CN)\}^+X^-$ have been found to be versatile synthetic intermediates in organoruthenium chemistry,[16] as one or both of the CH_3CN ligands may be readily replaced by another ligand. Thus, in addition to being a product of Cl substitution with an N donor ligand in our studies, a complex such as $\{(\eta^6\text{-}C_6H_6)Ru(TMNA)(CH_3CN)\}^+PF_6^-$ could serve as a precursor for other ligand substitution products (vide infra), whereas the benzylamine analogue, $\{(\eta^6\text{-}C_6H_6)Ru(TMBA)(CH_3CN)\}^+PF_6^-$, could not be isolated.[3] **2a,a′** reacts cleanly with $NaPF_6$ in CH_3CN solution to form $\{(\eta^6\text{-}C_6H_6)Ru(TMNA)(CH_3CN)\}^+PF_6^-$, **9c,c′**, which was isolated as a yellow microcrystalline product in 71.5% yield. This complex is only moderately stable and decomposes in solution over a 2 day period and in the solid state within a weak. ^1H and $^{13}C\{^1H\}$ NMR spectroscopy in acetone-d_6 shows the presence of two diastereomers in a 2.17:1 ratio (37% de). The ^1H and ^{13}C chemical shifts of the major and minor diastereomer are similar to those of **2a,a′**, respectively. Thus, we assign to the major diastereomer the (S_{Ru}, R_C) and to the minor diastereomer the (R_{Ru}, R_C) absolute configuration.

(16) (a) McCormick, F. B.; Cox, D. D.; Gleason, W. B. *Organometallics* **1993**, *12*, 610. (b) Seddon, E. A.; Seddon, K. R. *The Chemistry of Ruthenium*; Elsevier: Amsterdam, 1984; Chapter 9.

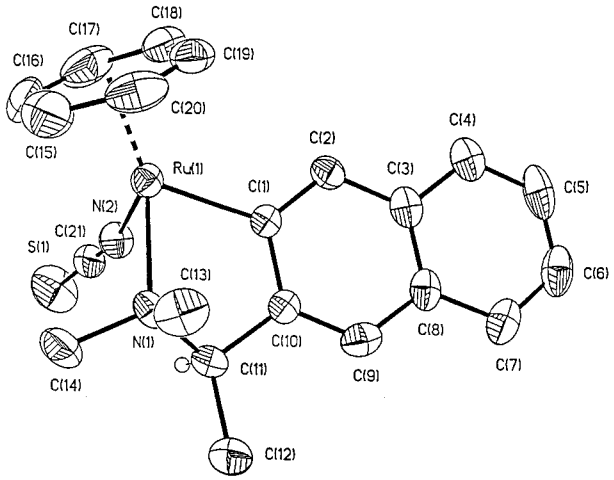

Figure 8. Structural drawing of **7b**, showing the atom-numbering scheme (40% probability ellipsoids, the hydrogen atom has an arbitrary radius of 0.1 Å). Selected bond lengths (Å) and angles (deg) are Ru(1)−C(1), 2.064(4); Ru(1)−C(arene, av), 2.208(6); Ru(1)−N(2), 2.071(4); Ru(1)−N(1), 2.176(3); N(2)−C(21), 1.144(6); C(21)−S(1), 1.635(5); C(1)−Ru(1)−N(1), 78.8(2); C(1)−Ru(1)−N(2), 86.9(2); N(1)−Ru(1)−N(2), 85.9(2); Ru(1)−N(2)−C(21), 167.7(4); N(2)−C(21)−S(1), 179.4(4).

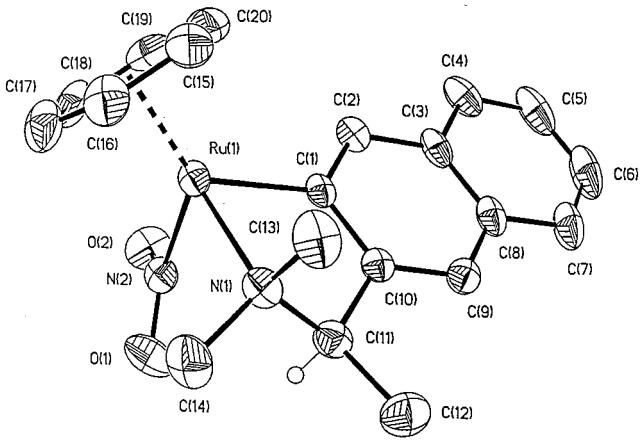

Figure 9. Structural drawing of **8b**, showing the atom-numbering scheme (40% probability ellipsoids, the hydrogen atom has an arbitrary radius of 0.1 Å). Selected bond lengths (Å) and angles (deg) are Ru(1)−C(1), 2.073(4); Ru(1)−C(arene, av), 2.231(16); Ru(1)−N(2), 2.083(4); Ru(1)−N(1), 2.201(5); N(2)−O(1), 1.232(6); N(2)−O(2), 1.242(5); C(1)−Ru(1)−N(1), 78.1(2); C(1)−Ru(1)−N(2), 85.9(2); N(1)−Ru(1)−N(2), 92.7(3); Ru(1)−N(2)−O(1), 124.4(3); Ru(1)−N(2)−O(2), 117.9(4); O(1)−N(2)−O(2), 117.6(5).

B. L = Pyridine, 10c,c′. The reaction of **2a,a′** with pyridine in the presence of $NaPF_6$ in CH_2Cl_2/EtOH-

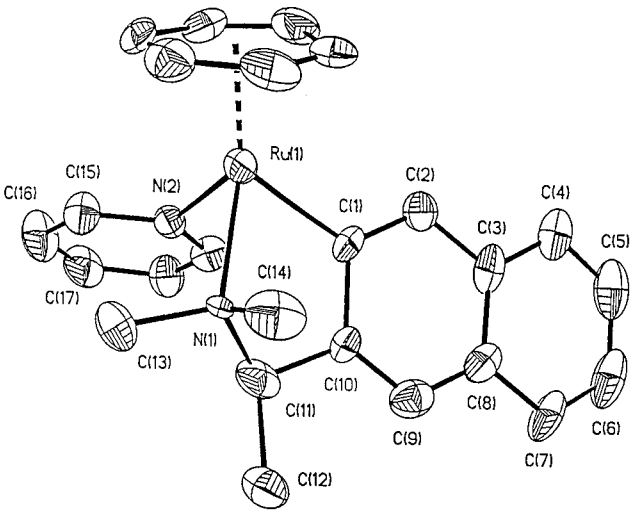

Figure 10. Structural drawing of **10c**, showing the atom-numbering scheme (40% probability ellipsoids). Selected bond lengths (Å) and angles (deg) are Ru(1)−C(1), 2.04(1); Ru(1)−C(arene, av), 2.22(1); Ru(1)−N(2), 2.174(8); Ru(1)−N(1), 2.156(7); C(1)−Ru(1)−N(1), 77.3(4); C(1)−Ru(1)−N(2), 87.7(3); N(1)−Ru(1)−N(2), 86.3(3).

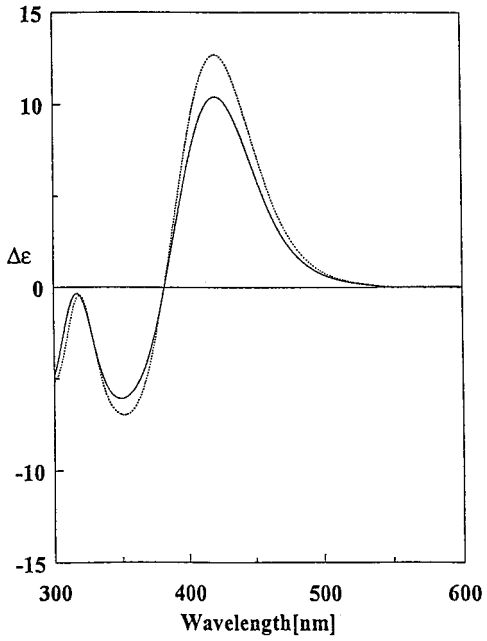

Figure 11. CD spectra of **10c,c′** (··· 64.2% de) and **11c,c′** (— 63.6% de) in CH_2Cl_2, 1.8×10^{-4} M, 1 cm path length.

(100%) (1:20) yielded a yellow microcrystalline product in 75% yield whose ^{1}H NMR spectrum in acetone-d_6 indicated the presence of two diastereomers in a 4.6:1 ratio (64.2% de). These two diastereomers, (S_{Ru}, R_C)- and (R_{Ru}, R_C)-[(η^6-C_6H_6) Ru(TMNA)(Py)]$^+PF_6^-$, are designated **10c,c′** respectively. Crystallization of the mixture from CH_2Cl_2/Et_2O−hexane (1:1) with slow diffusion of the solvents over several days afforded golden rod-shaped crystals. The ^{1}H NMR spectrum of these crystals in CD_3NO_2 showed the presence of two diastereomers in a 14.4:1 ratio. An X-ray crystallographic study, conducted on a suitable single crystal from this sample, showed (Figure 10) the structure to be **10c** with an (S_{Ru}, R_C) absolute configuration. The metrical parameters are very similar to those of both **2a**, the chloride precursor, and the benzylamine analogue[3] (R_{Ru}, S_C)-[(η^6-C_6H_6) Ru(TMBA)(Py)]$^+BPh_4^-$. The Ru−N(1) (2.156(7) Å) and Ru−N(2) (2.174(8) Å) distances are slightly shorter and longer than those in the benzylamine analogue (2.193(3), 2.148(9) Å, respectively).

The CD spectrum (Figure 11) of the bulk crude sample shows the same morphology as that of the chloride complex precursor, **2a**. Thus, the absolute configuration of the major diastereomer, **10c**, is (S_{Ru}, R_C), and this substitution reaction proceeds with predominant retention of configuration at Ru.

C. L = 4-Methylpyridine (4-Me-py), 11c,c′. The reaction of **2a,a′** with 4-methylpyridine in the presence of $NaPF_6$ in CH_2Cl_2/EtOH (100%) (1:30) yielded an orange microcrystalline product in 80% yield whose ^{1}H NMR spectrum in acetone-d_6 indicated the presence of two diastereomers in a 4.5:1 ratio (63.6% de). Crystallization of the mixture in the same manner as for the pyridine analogue afforded orange plates. The ^{1}H NMR spectrum in $CDCl_3$ showed the presence of two diastereomers in 14:1 ratio. An X-ray structure of a suitable single crystal (Figure 12) showed that the major diastereomer has the (S_{Ru}, R_C) absolute configuration, **11c**. The metrical parameters are very similar to those of **2a, 10c**, and the benzylamine analogue[3] (S_{Ru}, R_C)-[(η^6-

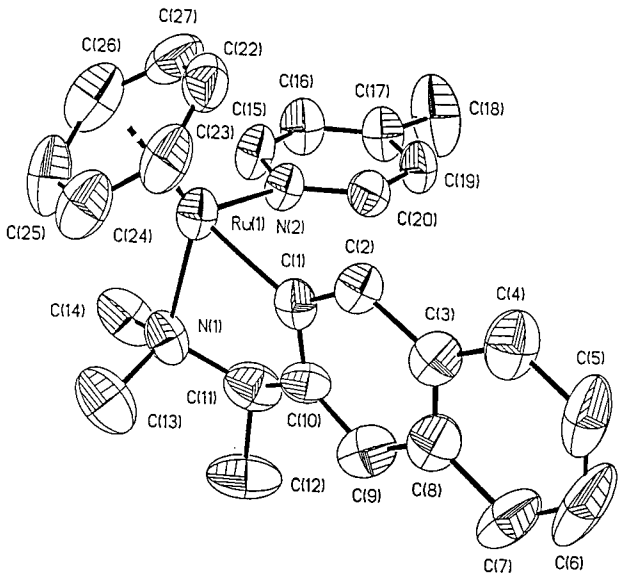

Figure 12. Structural drawing of **11c**, showing the atom-numbering scheme (40% probability ellipsoids). Selected bond lengths (Å) and angles (deg) are Ru(1)−C(1), 2.08(1); Ru(1)−C(arene, av), 2.23(1); Ru(1)−N(2), 2.151(8); Ru(1)−N(1), 2.182(8); C(1)−Ru(1)−N(1), 78.7(5); C(1)−Ru(1)−N(2), 87.4(3); N(1)−Ru(1)−N(2), 89.2(3).

C_6H_6)- Ru(TMBA)(4-Me-Py)]$^+BPh_4^-$. As was observed for the benzylamine complexes[3] of pyridine and 4-methylpyridine, and also for the naphthylamine complexes, the Ru−N (4-Me-py) bond length of 2.151(8) Å is slightly shorter than the Ru−N (py) bond length of 2.174(8) Å. For both pairs of complexes, this indicates a slightly stronger bond in the 4-Me-py complexes.

The CD spectra of the bulk crude samples of the pyridine and 4-methylpyridine complexes (Figure 11) are nearly superimposable, and both have the same morphology as that of the chloride complex precursor, **2a**. Thus, the absolute configuration of the major diastereomer, **11c**, is (S_{Ru}, R_C), and this substitution

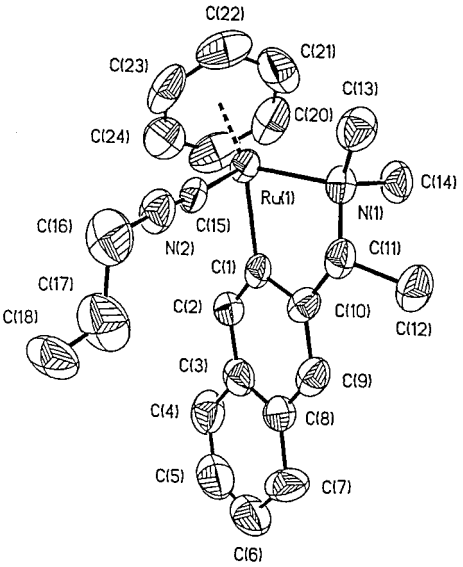

Figure 13. Structural drawing of **12c**, showing the atom-numbering scheme (40% probability ellipsoids). Selected bond lengths (Å) and angles (deg) are Ru(1)−C(1), 2.078-(7); Ru(1)−C(arene, av), 2.23(1); Ru(1)−C(15), 1.929(7); Ru(1)−N(1), 2.167(6); C(15)−N(2), 1.166(9); N(2)−C(10), 1.44(1); C(16)−C(17), 1.49(2); C(17)−C(18), 1.11(2); C(1)−Ru(1)−N(1), 78.4(2); C(1)−Ru(1)−C(15), 82.5(3); N(1)−Ru(1)−C(15), 90.0(3); Ru(1)−C(15)−N(2), 176.4(6); C(15)−N(2)−C(16), 176.3(10).

reaction proceeds with predominant retention of configuration at Ru.

D. L = Allylisonitrile, C≡NCH$_2$CH=CH$_2$ (12c). The reaction of **2a,a′** with allylisonitrile[17] in the presence of $NaPF_6$ in CH_2Cl_2/EtOH (100%) (1:30) yielded a yellow microcrystalline product in 80% yield. The ^{1}H and ^{13}C{^{1}H} NMR spectrum in acetone-d_6 indicated the presence of a single diastereomer. The^{1}H and ^{13}C chemical shifts were assigned by a combination of selective proton decoupling, COSY, APT, and HETCOR experiments.

The crystal structure, in which C_{18} and the PF_6 anion are disordered over two sites (Figure 13), and the CD spectrum show that this diastereomer has the (S_{Ru}, R_C) absolute configuration. Thus, this substitution reaction proceeds with predominant retention of configuration at Ru.

4. Substitution of Cl by Phosphines: Synthesis and Characterization of {(η^6-C$_6$H$_6$)Ru[C$_{10}$H$_6$CH(Me)NMe$_2$](R$_3$P)}$^+$PF$_6^-$. A. R$_3$P = Ph$_3$P, 13c,c′. This compound was synthesized from two different precursors (Scheme 3). The reaction of **2a,a′** with excess Ph_3P in the presence of $NaPF_6$ in CH_2Cl_2/EtOH (100%) (1:30) yielded a yellow-orange microcrystalline solid in 75% yield. The ^{31}P{^{1}H} NMR spectrum of this material in acetone-d_6 showed singlet resonances at δ 30.78 and 23.98 (Ph_3P=O) and a septet at $\delta = -144.99$ ppm (PF_6^-, $^1J_{PF} = 707.8$ Hz). The ^{1}H and ^{13}C{^{1}H} NMR spectra of this sample showed the presence of a single diastereomer. The reaction of **9c,c′** (2.17−1 ratio, 37% de) with excess Ph_3P in CH_2Cl_2/EtOH (100%) (1:30) yielded a yellow-orange microcrystalline solid in 70% yield (43% after crystallization and separation of the crystallized product). The ^{31}P{^{1}H} NMR spectrum of the crude material in acetone-d_6 showed the presence of three singlets at δ 31.95, 30.79 (1:4 ratio), and 23.93 ppm (Ph_3P=O) and a septet at $\delta = -144.99$ ppm (PF_6^- $^1J_{PF} = 707.8$ Hz). The ^{1}H and ^{13}C{^{1}H} NMR spectra of this material in acetone-d_6 showed the presence of two diastereomers in a 1:4 ratio (60% de).

Scheme 3

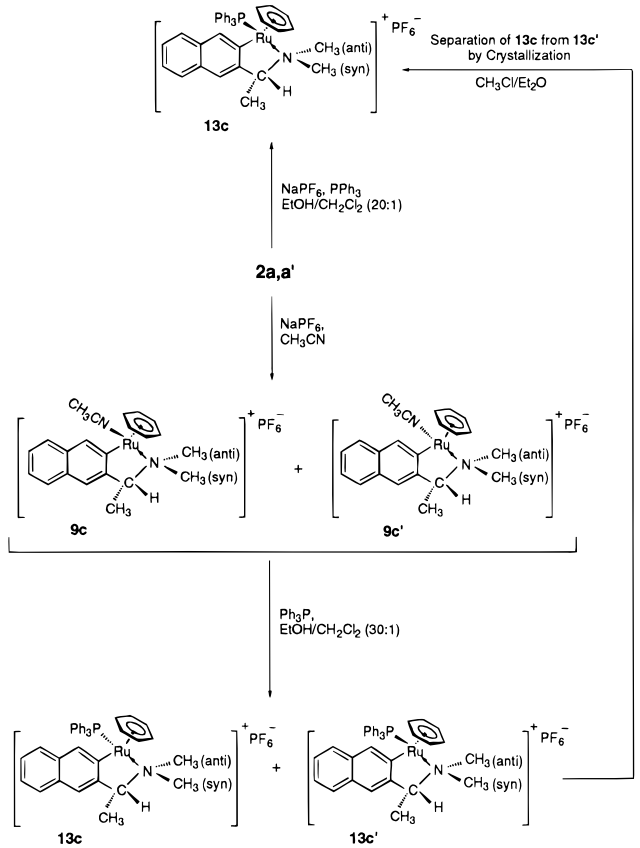

Single crystals from each reaction were obtained from $CHCl_3$/Et_2O−hexane (1:1), and in both cases the ^{31}P-{^{1}H} NMR spectra in acetone-d_6 showed a singlet at δ 30.77 ppm and a septet at $\delta = -145.02$ ppm (PF_6^-, $^1J_{PF} = 707.8$ Hz) in a 1:1 ratio.

The crystal structures of the two crystals are isomorphous and isostructural; both crystallize as $CHCl_3$ solvates (Figure 14 shows one of them) with (S_{Ru}, R_C) and Ph_3P (M)[18] absolute configuration. The conformation of the five-membered chelate ring is the same as that in **2a**, and the metrical parameters are similar to those of the benzylamine analogue[3] including the Ru−P distances (2.386(3) Å **13c**, 2.377(3) Å av for the benzylamine analogue). The substitution reaction of the chloride complex **2a** proceeds with predominant retention of configuration at Ru, but considerable inversion of configuration for the minor diastereomer occurs in the substitution of the CH_3CN ligand in **9c,c′**. The ratios of the diastereomers are quite different in these two substitution reactions, and these diastereomers do not interconvert in solution, demonstrating that the diastereoselectivity of these ligand substitution reactions is under kinetic control.

(17) Schöllkopf, U.; Jentsch, R.; Madawinata, K.; Harms, R. *Liebigs Ann. Chem.* **1976**, 2105.

(18) Eliel, E. L.; Wilen, S. H. In *Stereochemistry of Organic Compounds*; Wiley: New York, 1994.

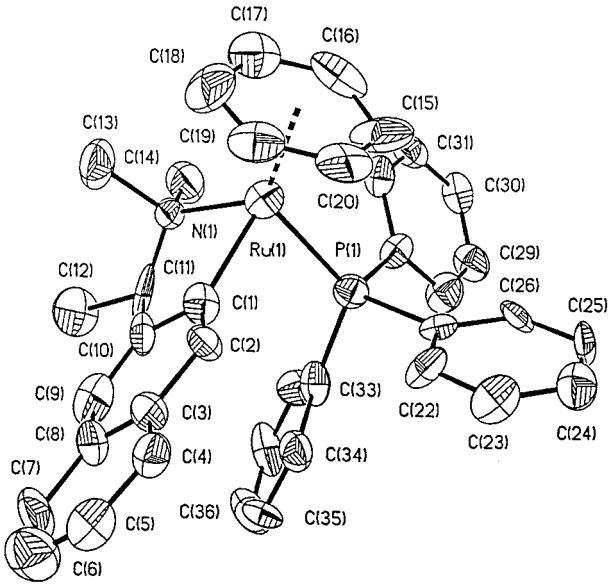

Figure 14. Structural drawing of **13c**, showing the atom-numbering scheme (40% probability ellipsoids). Selected bond lengths (Å) and angles (deg) are Ru(1)−C(1), 2.07(2); Ru(1)−C(arene, av), 2.27(2); Ru(1)−P(1), 2.371(4); Ru(1)−N(1), 2.12(1); C(1)−Ru(1)−N(1), 76.8(5); C(1)−Ru(1)−P(1), 88.4(5); N(1)−Ru(1)−P(1), 94.5(3).

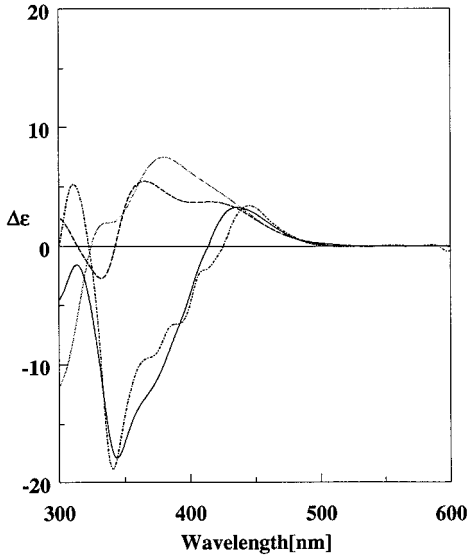

Figure 15. CD spectra of **13c,c′** (—·—·—·, 60% de), **14c,c′** (—, 48% de), **15c,c′** (···, 20% de) and **16c,c′** (- - -, 16% de) in CH_2Cl_2 (**13c,c′**, **14c,c′**, and **16c,c′** 4.4×10^{-4} M, **15c,c′**, 4.4×10^{-5} M), 1 cm path length.

The CD spectrum of the bulk crude sample from the CH_3CN reaction (Figure 15) has the same morphology as that for **2a**, consistent with the NMR spectral data that the major diastereomer has the (S_{Ru}, R_C) absolute configuration.

B. R_3P = 1-Phenyldibenzophosphole (PDBP), 14c,c′. The reaction of **2a,a′** with excess PDBP[19] in the presence of $NaPF_6$ in CH_2Cl_2/EtOH (100%) (1:30) yielded a yellow microcrystalline solid in 70% yield. The $^{31}P\{^1H\}$ NMR spectrum of this material in $CDCl_3$ showed singlets at δ 28.67 and 28.17 ppm (2.85:1 ratio, 48% de) and a septet at $\delta = -144.98$ ppm (PF_6^-, $^1J_{PF} = 707.4$ Hz). The ^1H and $^{13}C\{^1H\}$ NMR spectra of this sample in acetone-d_6 showed the presence of two diastereomers in a 2.85:1 ratio. Single crystals were obtained from acetone/ether−hexane (1:1), and the $^{31}P\{^1H\}$ NMR spectrum of these crystals in acetone-d_6 showed a singlet at δ 28.67 ppm and a septet at $\delta = -144.98$ ppm (PF_6^-, $^1J_{PF} = 707.4$ Hz) in a 1:1 ratio. The ^1H NMR spectrum of these crystals in acetone-d_6 showed the presence of a single diastereomer.

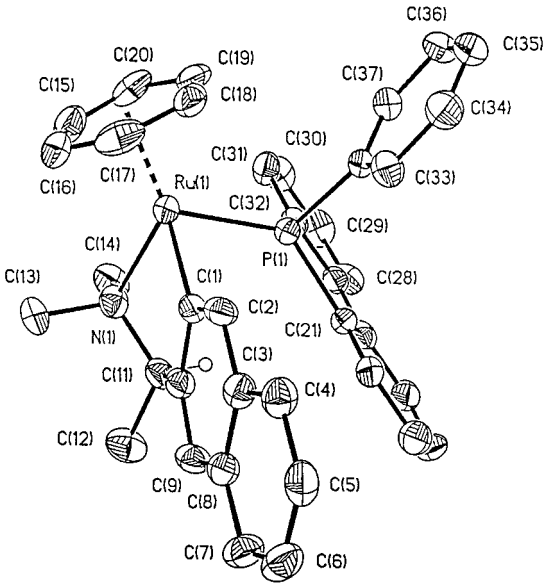

Figure 16. Structural drawing of **14c**, showing the atom-numbering scheme (40% probability ellipsoids, the hydrogen atom has an arbitrary radius of 0.1 Å). Selected bond lengths (Å) and angles (deg) are Ru(1)−C(1), 2.061(6); Ru(1)−C(arene, av), 2.254(8); Ru(1)−P(1), 2.231(1); Ru(1)−N(1), 2.197(4); C(7)−Ru(1)−N(1), 78.3(2); C(1)−Ru(1)−P(1), 85.0(2); N(1)−Ru(1)−P(1), 96.0(1).

The crystal structure (Figure 16) shows that this compound has the (S_{Ru}, R_C) absolute configuration; the five-membered chelate ring possesses the puckered envelope conformation with the CCH_3 group pseudoequatorial. The metrical parameters are similar to those of **2a** and the benzylamine analogue.[3] As for the benzylamine analogue, the Ru−P bond distance (2.331(1) Å) is slightly shorter than that in the PPh_3 compound **9c** (2.386(3) Å).

The CD spectrum of the bulk mixture of diastereomers (Figure 15) has the same morphology as that of **2a**, consistent with the major diastereomer having the (S_{Ru}, R_C) absolute configuration. Thus, this substitution reaction proceeds with predominant retention of configuration at Ru.

C. R_3P = 1-Phenyl-3,4-dimethylphosphole (DMPP), 15c,c′. The reaction of **2a,a′** with a slight excess of DMPP[20] in the presence of $NaPF_6$ in CH_2Cl_2/EtOH (100%) (1:30) produced an orange microcrystalline solid in 65% yield. The $^{31}P\{^1H\}$ NMR spectrum of this material in acetone-d_6 showed the presence of two singlets at δ 42.72 and 34.48 ppm (1:1.5 ratio, 20% de) and a septet at $\delta = -144.98$ ppm (PF_6^-, $^1J_{PF} = 707.4$ Hz). The ^1H and $^{13}C\{^1H\}$ NMR spectra of this sample in acetone-d_6 also show the presence of two diastereomers in the same ratio. Single crystals, as orange plates,

(19) Affandi, S.; Green, R. L.; Hsieh, B. T.; Holt, M. S.; Nelson, J. H.; Alyea, E. C. *Synth. React. Inorg. Met.-Org. Chem.* **1987**, *17*, 307.

(20) Breque, A.; Mathey, F.; Savignac, P. *Synthesis* **1981**, 983.

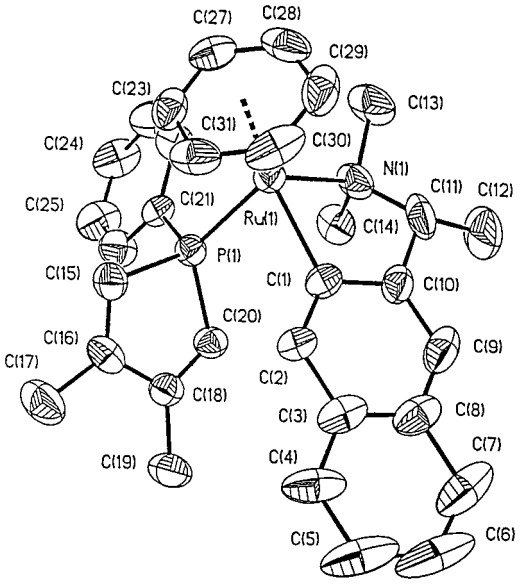

Figure 17. Structural drawing of **15c′**, showing the atom-numbering scheme (40% probability ellipsoids). Selected bond lengths (Å) and angles (deg) are Ru(1)−C(1), 2.073(7); Ru(1)−C(arene, av), 2.261(9); Ru(1)−P(1), 2.348(2); Ru(1)−N(1), 2.221(6); C(1)−Ru(1)−N(1), 77.6(3); C(1)−Ru(1)−P(1), 85.7(2); N(1)−Ru(1)−P(1), 95.8(2).

of the minor diastereomer were obtained from CH_2Cl_2/Et_2O−hexane (1:1). The $^{31}P\{^1H\}$ NMR spectrum of these crystals in acetone-d_6 showed a singlet at δ 42.71 ppm and a septet at $\delta = -144.98$ ppm (PF_6^-, $^1J_{PF} = 707.4$ Hz) in a 1:1 ratio. The ^1H and $^{13}C\{^1H\}$ NMR spectra of this sample in acetone-d_6 showed the presence of a single diastereomer.

The crystal structure (Figure 17) shows that the compound has the (R_{Ru}, R_C) absolute configuration. The five-membered chelate ring is puckered with the envelope conformation, and the CCH_3 group is pseudoequatorial. The Ru−P distance (2.348(2) Å) is slightly shorter and longer, respectively, than those observed for the PPh_3 (**13c**, 2.386(3) Å) and PDBP (**14c**, 2.331(1) Å) analogues.

The CD spectrum of the bulk mixture of diastereomers (Figure 15) has the same morphology as that of **2a**, consistent with the major diastereomer having the (S_{Ru}, R_C) absolute configuration. Thus, this substitution reaction proceeds with predominant retention of configuration at Ru.

D. R_3P = Et_3P, 16c,c′. The reaction of **2a,a′** with a slight excess of Et_3P in the presence of $NaPF_6$ in CH_2Cl_2/EtOH (100%) (1:30) produced an orange microcrystalline solid in 78% yield. The $^{31}P\{^1H\}$ NMR spectrum of this material in acetone-d_6 shows singlets at δ 19.05 and 16.60 ppm (1:1.4 ratio, 20% de) and a septet at $\delta = -145.00$ ppm (PF_6^-, $^1J_{PF} = 713$ Hz). The ^1H and $^{13}C\{^1H\}$ NMR spectra of this sample in acetone-d_6 also show the presence of two diastereomers in the same ratio. Single crystals, as orange blocks, of the minor diastereomer were obtained from CH_2Cl_2/Et_2O−hexane (1:1). The $^{31}P\{^1H\}$ NMR spectrum of these crystals in $CDCl_3$ showed a singlet at δ 18.98 ppm and a septet at $\delta = -145.00$ ppm (PF_6^-, $^1J_{PF} = 707.5$ Hz) in a 1:1 ratio. The ^1H and $^{13}C\{^1H\}$ NMR spectra of these crystals in acetone-d_6 also showed the presence of a single diastereomer.

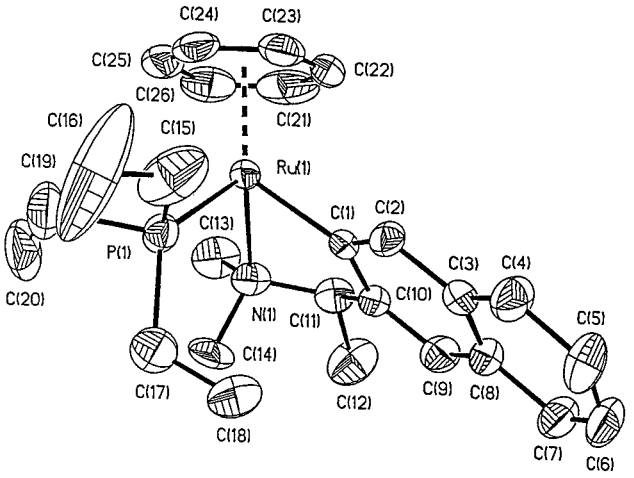

Figure 18. Structural drawing of **16c′**, showing the atom-numbering scheme (40% probability ellipsoids). Selected bond lengths (Å) and angles (deg) are Ru(1)−C(1), 2.067(6); Ru(1)−C(arene, av), 2.25(1); Ru(1)−P(1), 2.364(2); Ru(1)−N(1), 2.231(7); C(1)−Ru(1)−N(1), 77.4(3); C(1)−Ru(1)−P(1), 88.0(2); N(1)−Ru(1)−P(1), 98.7(2).

The crystal structure (Figure 18) shows that the compound has the (R_{Ru}, R_C) absolute configuration. The five-membered chelate ring has the puckered envelope conformation, and the CCH_3 group is pseudoequatorial. The Ru−P distance (2.364(2) Å) is comparable to that observed for the DMPP complex (**15c′**, 2.348(2) Å).

The CD spectrum of the bulk mixture of diastereomers (Figure 15) has the same morphology as that of **2a**, consistent with the major diastereomer having the (S_{Ru}, R_C) absolute configuration.

5. Trends in NMR Chemical Shifts and Their Relation to Diastereomer Absolute Configuration. The absolute configurations of the diastereomers can be determined by NMR spectroscopy on the basis of the considerable database that is now available for the TMBA[1,3] and TMNA complexes. For both series of complexes, when two diastereomers can be detected, the proton chemical shifts for the H_1 and (η^6-C_6H_6) moiety of the (S_{Ru}, R_C) diastereomers are always more downfield and those of the CCH_3 group are always more upfield of those of the same resonances for the (R_{Ru}, R_C) diastereomers. The carbon chemical shifts of C_1 and the CCH_3 group for the (S_{Ru}, R_C) diastereomer are always more upfield than those for the (R_{Ru}, R_C) diastereomer, while the reverse is true for the carbon chemical shifts of the (η^6-C_6H_6) moiety. For the phosphine complexes, the phosphorus chemical shifts of the (S_{Ru}, R_C) diastereomer are always more downfield than those of the (R_{Ru}, R_C) diastereomers. The diastereomeric ratio may be determined from the relative integrated intensities of any of these pairs of resonances.

6. Reactions of 2a,a′ with Alkynes. Since [(η^6-C_6H_6)-Ru(TMBA)Cl] reacts[21] with internal alkynes and $NaPF_6$ to form novel Ru(0) complexes of the type [(η^6-C_6H_6)Ru(η^4-$C_6H_4CH(Me)NMe_2CR^1{=}CR^2$ -1,2)]$^+PF_6^-$, we have probed the reactions of **2a,a′** with selected alkynes.

(21) (a) Abbenins, H. C. L.; Pfeffer, M.; Sutter, J.-P.; de Cian, A.; Fischer, J.; Ji, H.-L.; Nelson, J. H. *Organometallics* **1993**, *12*, 4404. (b) Pfeffer, M.; Sutter, J.-P.; Urriolabeitia, E. P. *Inorg. Chim. Acta* **1996**, *249*, 63. (c) Ferstl, W.; Sakodinskaya, I. K.; Beydoun, N.; Le Borgne, G.; Pfeffer, M.; Ryabov, A. D. *Organometallics* **1997**, *16*, 411. (d) Pfeffer, M.; Sutter, J.-P.; Urriolabeitia, E. P. *Bull. Soc. Chim. Fr.* **1997**, *134*, 947.

Table 3. Diastereoselectivities and the Stereochemical Course of Cl^- Substitution Reactions of 2a,a′

compounds	diastereo-selectivity, % de	reacn stereochem at Ru[a] (% retention for major species)
	(i)	
2a,a′ (X = Cl)	92	N/A
3b,b′ (X = Br)	93.3	retention (100)
4b,b′ (X = I)	94.9	retention (100)
5b (X = N_3)	100	retention (100)
6b (X = NCO, N bound)	100	retention (100)
7b (X = NCS, N bound)	100	retention (100)
8b (X = NO_2, N bound)	100	retention (100)
	(ii)	
9c,c′ (L = $NCCH_3$)	37	retention (71)
10c,c′ (L = Py)	64.2	retention (86)
11c,c′ (L = 4-Me-Py)	63.6	retention (85)
12c (L = $CNCH_2CH{=}CH_2$)	100	retention (100)
13c,c′ (L = Ph_3P)	100, 60[b]	retention (100)
14c,c′ (L = PDBP)	48	retention (77)
15c,c′ (L = DMPP)	20	retention (63)
16c,c′ (L = Et_3P)	16	retention (60)

[a] The predominant stereochemical outcome, since some inversion also takes place; for the bromide and iodide reactions, the minor diastereomer undergoes 17% and 36% inversion, respectively. [b] Formed from **9c,c′**.

2a,a′ was reacted with PhC≡CH, MeC≡CPh, PhC≡CPh, $MeCO_2C{\equiv}CCO_2Me$, $LiC{\equiv}CC(CH_3)_3$, and LiC≡CPh in both CH_2Cl_2 and CH_3OH solutions in the presence and absence of $NaPF_6$. In all cases deep red solutions were formed that eventually turned greenish black, depositing elemental ruthenium. No characterizable products could be obtained from any of these reaction mixtures.

7. Diastereoselectivities of the Ligand Substitution Reactions and Comparisons with those of the Benzylamine Analogue. The results of our studies on the stereochemistry of Cl^- substitution reactions of **2a,a′** are summarized in Table 3. They clearly show that these reactions proceed with predominant retention of configuration at Ru. A search through the literature related to this subject[2,3,11] reveals that retention of configuration at the metal center has been the most common stereochemical outcome in these studies. While epimerization and/or racemization is sometimes observed, net inversion of metal configuration appears to be rare.

Table 4 lists comparative diastereoselectivities for chloride substitutions by a variety of ligands in the TMBA and TMNA analogues. For both series of complexes predominant retention of configuration was observed. Also for both series of complexes the diastereoselectivity generally increases with increasing steric bulk of the incoming ligand. The diastereoselectivity of the chloride substitutions is generally greater for the substitutions of the TMNA complex than for the TMBA analogue. To assess whether this has an electronic origin, the redox potentials for the Ru(II)/(III) couples were determined by cyclic voltammetry (Figure 19). For both complexes the Ru(II)/(III) couples are both chemically and electrochemically reversible processes. As can be seen from this figure, except for differences in the amplitude of the currents, because of differences in the concentrations of the two complexes, the two cyclic voltammograms are superimposable. Hence, within experimental error the redox potentials of the two

Table 4. Comparative Diastereoselectivities[a] of Cl^- Substitution Reactions of [(R)(TMBA)Ru(η^6-C_6H_6)Cl][b] and [(R)(TMNA)Ru(η^6-C_6H_6)Cl][c]

X	diastereoselectivity (% de) [(R)(TMBA)Ru(η^6-C_6H_6)Cl]	[(R)(TMNA)Ru(η^6-C_6H_6)Cl]
halides		
Cl	90.4	92
Br	93.2	93.3
I	94.3	94.9
P-donor ligands		
Ph_3P	60	100
diphos	57.4	N/A
PDBP	33.3	48
Et_3P	25.9	16
DMPP	13	20
N-donor ligands		
N_3	N/A	100
NCO	N/A	100
NCS	N/A	100
NO_2	N/A	100
4-Me-Py	51.2	63.6
Py	42.9	64.2
CH_3CN	N/A	37
C-donor ligand		
$CNCH_2CH{=}CH_2$	N/A	100

[a] % de = (% major diastereomer - % minor diastereomer). [b] Reference 3. [c] This work.

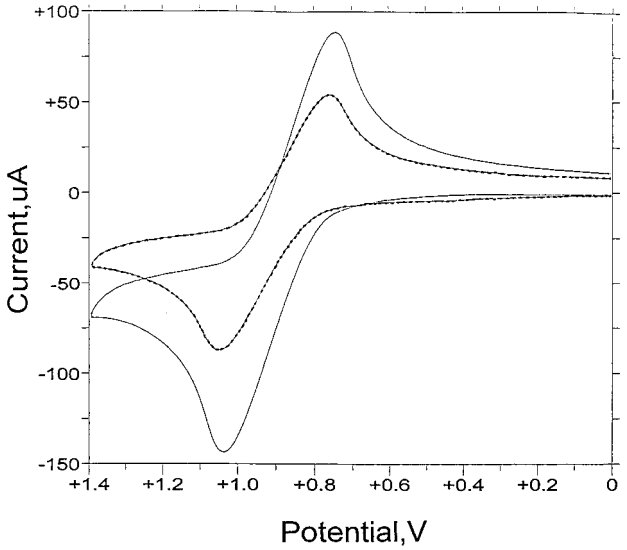

Figure 19. Cyclic voltammograms of (S_{Ru}, R_C)-[(η^6-C_6H_6)-Ru(TMBA)Cl] (—) and (S_{Ru}, R_C)-[(η^6-C_6H_6)Ru(TMNA)Cl] (•—•—•) in CH_2Cl_2 (25 °C) with 0.1 M n-Bu_4NPF_6 as supporting electrolyte. Potentials are vs an Ag/AgCl (aqueous) reference electrode.

complexes are the same. This implies[22] that there is no perceptible difference in the electronic donor or acceptor properties of the TMNA and TMBA ligands. Thus, by Ockham's Razor,[23] we suggest that the differences in the diastereoselectivities of the chloride substitution reactions for the two series of complexes have a steric origin. For the TMBA complexes the five-membered chelate ring is flexible and interconverts in solution between two limiting conformations wherein the CCH_3 group is either pseudoaxial or pseudoequatorial. For the TMNA complexes the five-membered chelate ring is

(22) Lever, A. B. P. *Inorg. Chem.* **1990**, *29*, 1271.
(23) Hoffmann, R.; Minkin, V. I.; Carpenter, B. K. *Bull. Soc. Chim. Fr.* **1996**, *133*, 117.

rigid and the CCH_3 group is always pseudoequatorial. This probably emanates from the larger naphthyl than phenyl ring systems. For the former, more mass, including solvent molecules, must be moved in order for λ- to δ- or vice versa ring conformational interchange to occur. This gives rise to a greater differentiation in steric buttressing toward the approach of an incoming ligand for the chloride substitution reactions in the TMNA complex than in the TMBA complex and results in generally greater diastereoselectivity regardless of whether these reactions occur by an associative or dissociative mechanism.[3]

Experimental Section

1. Physical Measurements. NMR spectra were recorded on a Varian Unity Plus-500 FT NMR spectrometer operating at 500 MHz for ^{1}H, 202 MHz for ^{31}P, and 125 MHz for ^{13}C. Proton and carbon chemical shifts were referenced to residual solvent resonances, and phosphorus chemical shifts were referenced to an external 85% aqueous solution of H_3PO_4. All shifts to low field, high frequency are positive. FT-IR spectra were recorded on a Nicolet Protégé 460 spectrometer for the IR region (400−4000 cm^{-1}) as a mineral oil mull or as thin films on KBr windows (abbreviations: shp = sharp, sh = shoulder, st = strong, w = weak, br = broad). UV−visible spectra were recorded at (25 °C) on a Perkin-Elmer Lambda-11 UV−visible spectrophotometer with an appropriate concentration of a CH_2Cl_2 solution of each compound placed in a cuvette with a cell path length (b) of 1.00 cm. CD spectra were recorded at (25 °C) on a JASCO J-600 spectropolarimeter with a CH_2Cl_2 solution of each compound placed in a cell where b = 1.00 cm. Cyclic voltammograms were recorded at (25 °C) in freshly distilled CH_2Cl_2 containing 0.1 M tetrabutylammonium hexafluorophosphate using a BAS CV 50-W voltammetric analyzer. A three-electrode system was used. The working electrode was a platinum disk, and the reference electrode was Ag/AgCl (aqueous) separated from the cell by a luggin capillary. The Fc/Fc$^+$ couple occurred at 554 mV[24] under the same conditions. Melting points were determined on a Mel-Temp apparatus; all complexes decomposed at temperatures above 160 °C. Elemental analyses were performed by Galbraith Laboratories, Knoxville, TN.

2. Preparation of {(η^6-C_6H_6)Ru[$C_{10}H_6CH(Me)NMe_2$]Cl}, (2a,a′). A suspension containing [(η^6-C_6H_6)$RuCl_2$]$_2$[6] (2.08 g, 4.16 mmol) and (R)$_C$-[(TMNA)HgCl][5] (3.61 g, 8.32 mmol) in 200 mL of acetonitrile, which had been freshly distilled from CaH_2, was stirred at ambient temperature under a blanket of dry nitrogen for 12 h. The original dark orange-brown color gradually changed to orange-red, and a small amount of a yellow solid appeared in the solution. The dark orange solution was filtered by gravity, and the solvent was removed on a rotary evaporator. The dark red-brown residue was dissolved in a minimum amount of CH_2Cl_2 and subjected to filtration chromatography over a short (∼7 × 2 cm^2) column of alumina which had been packed with a mixture of hexane/ether (1:1) and was eluted with CH_2Cl_2. A very dark grayish band containing $HgCl_2$, elemental Ru, and organic impurities moved very slowly, and a red band moved with the solvent front. The dark red-orange eluate was collected, and the solvent was removed on a rotary evaporator. The resulting deep orange powder was washed with several small portions of the hexane/ether mixture and dried under vacuum to afford 2.4 g (70.5%) of a deep orange solid. Anal. Calcd for $C_{20}H_{22}ClNRu$: C, 58.20; H, 5.33; N, 3.39. Found: C, 58.05; H, 5.20; N, 3.46.

^{1}H NMR (500 MHz, $CDCl_3$): **2a** (major), δ 1.31 (d, $^3J(H_7H_{12})$ = 6.8 Hz, 3H, CH_3(12)), 2.49 (s, 3H, NCH_3(13)), 3.44 (s, 3H, NCH_3(14)), 4.56 (qd, $^3J(H_7H_{12})$ = 6.8 Hz, $^4J(H_6H_7)$ = 1.5 Hz, 1H, H_7), 5.41 (s, 6H, η^6-C_6H_6), 7.18 (d, $^4J(H_6H_7)$ = 1.5 Hz, 1H, H_6), 7.27 (ddd, $^3J(H_4H_5)$ = 8.0 Hz, $^3J(H_3H_4)$ = 6.8 Hz, $^4J(H_2H_4)$ = 1.3 Hz, 1H, H_4), 7.37 (ddd, $^3J(H_2H_3)$ = 8.0 Hz, $^3J(H_3H_4)$ = 6.8 Hz, $^4J(H_3H_5)$ = 1.3 Hz, 1H, H_3), 7.66 (dd, $^3J(H_4H_5)$ = 8.0 Hz, $^4J(H_3H_5)$ = 1.3 Hz, 1H, H_5), 7.74 (dd, $^3J(H_2H_3)$ = 8.0 Hz, $^4J(H_2H_4)$ = 1.3 Hz, 1H, H_2), 8.66 (s, 1H, H_1); **2a′** (minor), δ 1.40 (d, $^3J(H_7H_{12})$ = 7.0 Hz, 3H, CH_3(12)), 2.47 (s, 3H, NCH_3-(13)), 3.51 (s, 3H, NCH_3(14)), 3.98 (q, $^3J(H_7H_{12})$ = 7.0 Hz, 1H, H_7), 5.33 (s, 6H, η^6-C_6H_6), 7.25 (dd, $^3J(H_4H_5)$ = 8.0 Hz, $^3J(H_3H_4)$ = 6.8 Hz, 1H, H_4), 7.26 (s, 1H, H_6), 7.36 (dd, $^3J(H_2H_3)$ = 8.0 Hz, $^3J(H_3H_4)$ = 6.8 Hz, 1H, H_3), 7.70 (d, $^3J(H_4H_5)$ = 8.0 Hz, 1H, H_5), 7.72 (d, $^3J(H_2H_3)$ = 8.0 Hz, 1H, H_2), 8.16 (s, 1H, H_1). The relative intensities of the two H_1 resonances (24:1) established the 92% de. ^{13}C{^{1}H} NMR (125 MHz, $CDCl_3$): **2a** (major), δ 9.1 (C_{12}), 49.7 (C_{13}), 52.6 (C_{14}), 66.9 (C_{11}), 86.1 (η^6-C_6H_6), 121.2 (C_9), 123.5 (C_6), 124.8 (C_5), 126.1 (C_4), 127.4 (C_7), 131.3 (C_3), 133.1 (C_8), 134.9 (C_2), 149.6 (C_{10}), 164.6 (C_1); **2a′** (minor), δ 10.3 (C_{12}), 49.3 (C_{13}), 55.3 (C_{14}), 75.8 (C_{11}), 85.8 (η^6-C_6H_6), 120.0 (C_9), 123.3 (C_6), 124.9 (C_5), 126.4 (C_4), 127.6 (C_7), 131.1 (C_3), 133.9 (C_8), 136.7 (C_2), 148.5 (C_{10}), 172.2 (C_1). UV−vis (c = 1.8 × 10^{-4} M in CH_2Cl_2 at 25 °C): λ_{max}, nm (ϵ, L mol^{-1} cm^{-1}) 442 (1.4 × 10^3), 409 (1.2 × 10^3). CD, molecular ellipticity $[\theta]_\lambda$ (deg cm^2 $dmol^{-1}$), where $[\theta]_\lambda$ = 3300$(\Delta\epsilon)_\lambda$ and $(\Delta\epsilon)_\lambda$ is the measured CD quantity (in units of L mol^{-1} cm^{-1}) at a given wavelength; c = 1.8 × 10^{-4} M in CH_2Cl_2 at 25 °C: $[\theta]_{600}$ = 0, $[\theta]_{453}$ = +39478, $[\theta]_{350}$ = −39600.

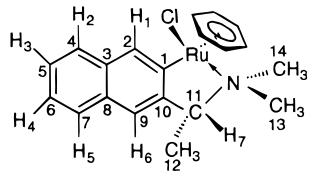

3. Synthesis and Characterization of the Products of Substitution Reactions {(η^6-C_6H_6)Ru[$C_{10}H_6CH(Me)NMe_2$]-(X)} (X = Br (3b,b′), I (4b,b′), N_3 (5b), NCO (6b), NCS (7b), NO_2 (8b)). The anion substitution products were all prepared by the same general method. This involved metathetic reactions of 2a,a′ with the appropriate sodium salt or AgNCO[10] in a mixture of CH_2Cl_2 and EtOH (95%). Reaction mixtures were not air sensitive, and no precautions were taken to exclude air. The reaction times for the N_3^-, NO_2^-, NCO^-, and NCS^- reactions were 2 h longer than those of the Br^- and I^- reactions. Since AgNCO is light sensitive, its reaction was performed in the dark. The following preparation of 3b,b′ is representative.

3b,b′ (X = Br). A sample of **2a,a′** (0.35 g, 0.85 mmol) was dissolved in 2.5 mL of CH_2Cl_2. To this solution was added a solution of 0.125 g (1.2 mmol) of NaBr in 80 mL of 95% EtOH. The resulting deep red transparent solution was stirred at ambient temperature for 4 h, after which the solvents were removed under reduced pressure. The orange solid residue was dissolved in a minimum amount of CH_2Cl_2 and subjected to filtration chromatography over a short (∼7 × 2 cm^2) column of alumina, which had been packed with a mixture of hexane/ether (1:1), and was eluted with CH_2Cl_2. This resulted in a very dark brown band (containing elemental Ru and organic impurities) at the top of the column and a red band, which moved with the solvent front. The red transparent eluate was collected and evaporated in vacuo. The resulting deep red powder was washed with several small portions of the hexane/ether mixture and filtered. Drying the resulting solid in vacuo gave the pure product as an orange-red, flaky solid, yield 0.325 g (85%). Anal. Calcd for $C_{20}H_{22}BrNRu$: C, 52.54; H, 4.81; N, 3.06. Found: C, 52.43; H, 4.72; N, 3.14. ^{1}H NMR (500 MHz, $CDCl_3$): **3b** (major), δ 1.32 (d, $^3J(H_7H_{12})$ = 6.5 Hz, 3H, CH_3(12)), 2.50 (s, 3H, NCH_3(13)), 3.50 (s, 3H, NCH_3(14)), 4.62 (qd, $^3J(H_7H_{12})$ = 6.5 Hz, $^4J(H_6H_7)$ = 1.0 Hz, 1H, H_7), 5.45 (s,

(24) Gagné, R. R.; Koval, C. A.; Lisensky, G. C. *Inorg. Chem.* **1980**, *19*, 2854.

6H, η^6-C_6H_6), 7.20 (d, $^4J(H_6H_7)$ = 1.0 Hz, 1H, H_6), 7.26 (ddd, $^3J(H_4H_5)$ = 8.0 Hz, $^3J(H_3H_4)$ = 6.5 Hz, $^4J(H_2H_4)$ = 1.0 Hz, 1H, H_4), 7.37 (ddd, $^3J(H_2H_3)$ = 8.0 Hz, $^3J(H_3H_4)$ = 6.5 Hz, $^4J(H_3H_5)$ = 1.0 Hz, 1H, H_3), 7.66 (dd, $^3J(H_4H_5)$ = 8.0 Hz, $^4J(H_3H_5)$ = 1.0 Hz, 1H, H_5), 7.73 (dd, $^3J(H_2H_3)$ = 8.0 Hz, $^4J(H_2H_4)$ = 1.0 Hz, 1H, H_2), 8.62 (s, 1H, H_1); **3b′** (minor), δ 1.41 (d, $^3J(H_7H_{12})$ = 6.5 Hz, 3H, CH_3(12)), 2.50 (s, 3H, NCH_3(13)), 2.45 (s, 3H, NCH_3(14)), 4.00 (q, $^3J(H_7H_{12})$ = 6.5 Hz, 1H, H_7), 5.42 (s, 6H, η^6-C_6H_6), 7.19 (s, 1H, H_6), 7.27 (ddd, $^3J(H_4H_5)$ = 8.0 Hz, $^3J(H_3H_4)$ = 6.5 Hz, $^4J(H_2H_4)$ = 1.0 Hz, 1H, H_3), 7.36 (ddd, $^3J(H_2H_3)$ = 8.0 Hz, $^3J(H_3H_4)$ = 6.5 Hz, $^4J(H_3H_5)$ = 1.0 Hz, 1H, H_4), 7.70 (d, $^3J(H_4H_5)$ = 8.0 Hz, 1H, H_5), 7.74 (d, $^3J(H_2H_3)$ = 8.0 Hz, 1H, H_2), 8.20 (s, 1H, H_1). The relative intensities of the two H_1 resonances (28.9:1) established the 93.3% de. $^{13}C\{^1H\}$ NMR (125 MHz, $CDCl_3$): **3b** (major), δ 9.3 (C_{12}), 49.7 (C_{13}), 53.7 (C_{14}), 68.0 (C_{11}), 86.2 (η^6-C_6H_6), 121.3 (C_9), 123.5 (C_6), 124.8 (C_5), 126.1 (C_4), 127.5 (C_7), 131.3 (C_3), 133.1 (C_8), 135.3 (C_2), 149.6 (C_{10}), 163.8 (C_1). UV−vis (c = 1.8 × 10^{-4} M in CH_2Cl_2 at 25 °C): λ_{max}, nm (ϵ, L mol^{-1} cm^{-1}) 450 (1.5 × 10^3), 415 (1.3 × 10^3). CD, c = 1.8 × 10^{-4} M in CH_2Cl_2 at 25 °C: λ_{max}, nm ($[\theta]_\lambda$, deg cm^2 $dmol^{-1}$) 600 (0), 459 (+48495), 374 (−55730).

4b,b′ (X = I): yield 0.324 g (88%). Anal. Calcd for $C_{20}H_{22}INRu$: C, 47.64; H, 4.36; N, 2.78. Found: C, 47.76; H, 4.45; N, 2.65. ^1H NMR (500 MHz, $CDCl_3$): **4b** (major), δ 1.33 (d, $^3J(H_7H_{12})$ = 7.0 Hz, 3H, CH_3(12)), 2.49 (s, 3H, NCH_3(13)), 3.54 (s, 3H, NCH_3(14)), 4.66 (q, $^3J(H_7H_{12})$ = 7.0 Hz, 1H, H_7), 5.49 (s, 6H, η^6-C_6H_6), 7.22(s, 1H, H_6), 7.24 (apparent t, $^3J(H_3H_4)$ = $^3J(H_4H_5)$ = 8.0 Hz, 1H, H_4), 7.37 (apparent t, $^3J(H_2H_3)$ = $^3J(H_3H_4)$ = 8.0 Hz, 1H, H_3), 7.67 (d, $^3J(H_4H_5)$ = 8.0 Hz, 1H, H_5), 7.71(d, $^3J(H_2H_3)$ = 8.0 Hz, 1H, H_2), 8.52 (s, 1H, H_1); **4b′** (minor), δ 1.39 (d, $^3J(H_7H_{12})$ = 6.5 Hz, 3H, CH_3(12)), 2.40 (s, 3H, NCH_3(13)), 3.67 (s, 3H, NCH_3(14)), 4.00 (q, $^3J(H_7H_{12})$ = 6.5 Hz, 1H, H_7), 5.42 (s, 6H, η^6-C_6H_6), 7.19 (s, 1H, H_6), 7.26 (apparent t, $^3J(H_3H_4)$ = $^3J(H_4H_5)$ = 8.0 Hz, 1H, H_4), 7.37 (apparent t, $^3J(H_2H_3)$ = $^3J(H_3H_4)$ = 8.0 Hz, 1H, H_3), 7.66 (d, $^3J(H_4H_5)$ = 8.0 Hz, 1H, H_5), 7.30 (d, $^3J(H_2H_3)$ = 8.0 Hz, 1H, H_2), 8.27 (s, 1H, H_1). The relative intensities of the two H_1 resonances (38.3:1) established the 94.9% de. $^{13}C\{^1H\}$ NMR (125 MHz, $CDCl_3$): **4b** (major), δ 9.5 (C_{12}), 49.3 (C_{13}), 55.6 (C_{14}), 70.0 (C_{11}), 86.5 (η^6-C_6H_6), 121.2 (C_9), 123.5 (C_6), 124.8 (C_5), 126.0 (C_4), 127.4 (C_7), 131.2 (C_3), 133.1 (C_8), 136.0 (C_2), 149.7 (C_{10}), 162.1 (C_1). UV−vis (c = 1.8 × 10^{-4} M in CH_2Cl_2 at 25 °C): λ_{max}, nm (ϵ, L mol^{-1} cm^{-1}) 470 (1.8 × 10^3), 428 (1.4 × 10^3). CD, c = 1.8 × 10^{-4} M in CH_2Cl_2 at 25 °C: λ_{max}, nm ($[\theta]_\lambda$, deg cm^2 $dmol^{-1}$) 600 (0), 469 (+47158), 385 (−76253), 322 (+12419).

5b (X = N_3): yield 0.156 g (75%). Anal. Calcd for $C_{20}H_{22}N_4Ru$: C, 57.24; H, 5.25; N, 13.36. Found: C, 57.31; H, 5.19; N, 13.24. ^1H NMR (500 MHz, acetone-d_6): δ 1.32 (d, $^3J(H_7H_{12})$ = 7.0 Hz, 3H, CH_3(12)), 2.82 (s, 3H, NCH_3(13)), 3.23 (s, 3H, NCH_3(14)), 3.99 (qd, $^3J(H_7H_{12})$ = 7.0 Hz, $^4J(H_6H_7)$ = 1.3 Hz, 1H, H_7), 5.54 (s, 6H, η^6-C_6H_6), 7.20 (d, $^4J(H_6H_7)$ = 1.3 Hz, 1H, H_6), 7.23 (ddd, $^3J(H_4H_5)$ = 8.0 Hz, $^3J(H_3H_4)$ = 6.5 Hz, $^4J(H_2H_4)$ = 1.3 Hz, 1H, H_4), 7.33 (ddd, $^3J(H_2H_3)$ = 8.0 Hz, $^3J(H_3H_4)$ = 6.5 Hz, $^4J(H_3H_5)$ = 1.3 Hz, 1H, H_3), 7.67 (dd, $^3J(H_4H_5)$ = 8.0 Hz, $^4J(H_3H_5)$ = 1.3 Hz, 1H, H_5), 7.75 (dd, $^3J(H_2H_3)$ = 8.0 Hz, $^4J(H_2H_4)$ = 1.3 Hz, 1H, H_2), 8.73 (s, 1H, H_1). $^{13}C\{^1H\}$ NMR (125 MHz, acetone-d_6): δ 9.4 (C_{12}), 49.6 (C_{13}), 52.5 (C_{14}), 67.2 (C_{11}), 85.6 (η^6-C_6H_6), 121.2 (C_9), 123.7 (C_6), 125.0 (C_5), 126.2 (C_4), 127.5 (C_7), 131.4 (C_3), 133.1 (C_8), 134.7 (C_2), 149.3 (C_{10}), 164.2 (C_1). IR (Nujol): ν_a (NNN) 2044 cm^{-1} (shp, st), ν_s (NNN) 1376 cm^{-1} (shp, w). UV−vis (c = 1.8 × 10^{-4} M in CH_2Cl_2 at 25 °C): λ_{max}, nm (ϵ, L mol^{-1} cm^{-1}) 416 (2 × 10^3), 393 (1.9 × 10^3). CD, c = 1.8 × 10^{-4} M in CH_2Cl_2 at 25 °C: λ_{max}, nm ($[\theta]_\lambda$, deg cm^2 $dmol^{-1}$) 600 (0), 458 (+47758), 367 (−79120), 317 (+4121).

6b (X = NCO): yield 0.166 g (80%). Anal. Calcd for $C_{21}H_{22}N_2ORu$: C, 60.15; H, 5.25; N, 6.68. Found: C, 60.01; H, 5.30; N, 6.57. ^1H NMR (500 MHz, acetone-d_6): δ 1.35 (d, $^3J(H_7H_{12})$ = 6.8 Hz, 3H, CH_3(12)), 2.52 (s, 3H, NCH_3(13)), 3.35 (s, 3H, NCH_3(14)), 4.13 (qd, $^3J(H_7H_{12})$ = 6.8 Hz, $^4J(H_6H_7)$ = 1.5 Hz, 1H, H_7), 5.53 (s, 6H, η^6-C_6H_6), 7.22 (d, $^4J(H_6H_7)$ = 1.5 Hz, 1H, H_6), 7.24 (ddd, $^3J(H_4H_5)$ = 8.0 Hz, $^3J(H_3H_4)$ = 6.5 Hz, $^4J(H_2H_4)$ = 1.0 Hz, 1H, H_4), 7.33 (ddd, $^3J(H_2H_3)$ = 8.0 Hz, $^3J(H_3H_4)$ = 6.5 Hz, $^4J(H_3H_5)$ = 1.0 Hz, 1H, H_3), 7.67 (dd, $^3J(H_4H_5)$ = 8.0 Hz, $^4J(H_3H_5)$ = 1.0 Hz, 1H, H_5), 7.73 (dd, $^3J(H_2H_3)$ = 8.0 Hz, $^4J(H_2H_4)$ = 1.0 Hz, 1H, H_2), 8.70 (s, 1H, H_1). $^{13}C\{^1H\}$ NMR (125 MHz, acetone-d_6): δ 9.7 (C_{12}), 49.5 (C_{13}), 53.1 (C_{14}), 68.4 (C_{11}), 87.4 (η^6-C_6H_6), 121.5 (C_9), 123.9 (C_6), 125.4 (C_5), 126.9 (C_4), 128.3 (C_7), 132.3 (C_3), 134.2 (C_8), 136.1 (C_2), 151.5 (C_{10}), 166.2 (C_1). IR (Nujol): ν_a (NCO) 2239 cm^{-1} (b, st), ν_s (NCO) 1336 cm^{-1} (w), δ (NCO) 624 cm^{-1} (w). UV−vis (c = 1.8 × 10^{-4} M in CH_2Cl_2 at 25 °C): λ_{max}, nm (ϵ, L mol^{-1} cm^{-1}) 412 (1.6 × 10^3), 337 (3.6 × 10^3). CD, c = 1.8 × 10^{-4} M in CH_2Cl_2 at 25 °C: λ_{max}, nm ($[\theta]_\lambda$, deg cm^2 $dmol^{-1}$) 600 (0), 429 (+44252), 343 (−38922), 320 (−25047).

7b (X = NCS): yield 0.163 g (74%). Anal. Calcd for $C_{21}H_{22}N_2SRu$: C, 57.93; H, 5.05; N, 6.43. Found: C, 57.74; H, 5.13; N, 6.29. ^1H NMR (500 MHz, acetone-d_6): δ 1.40 (d, $^3J(H_7H_{12})$ = 6.8 Hz, 3H, CH_3(12)), 2.57 (s, 3H, NCH_3(13)), 3.35 (s, 3H, NCH_3(14)), 4.00 (qd, $^3J(H_7H_{12})$ = 6.8 Hz, $^4J(H_6H_7)$ = 1.5 Hz, 1H, H_7), 5.67 (s, 6H, η^6-C_6H_6), 7.26 (ddd, $^3J(H_4H_5)$ = 8.0 Hz, $^3J(H_3H_4)$ = 6.8 Hz, $^4J(H_2H_4)$ = 1.0 Hz, 1H, H_4), 7.27 (d, $^4J(H_6H_7)$ = 1.5 Hz, 1H, H_6), 7.35 (ddd, $^3J(H_2H_3)$ = 8.0 Hz, $^3J(H_3H_4)$ = 6.8 Hz, $^4J(H_3H_5)$ = 1.5 Hz, 1H, H_3), 7.69 (dd, $^3J(H_4H_5)$ = 8.0 Hz, $^4J(H_3H_5)$ = 1.5 Hz, 1H, H_5), 7.74 (dd, $^3J(H_2H_3)$ = 8.0 Hz, $^4J(H_2H_4)$ = 1.0 Hz, 1H, H_2), 8.69 (s, 1H, H_1). $^{13}C\{^1H\}$ NMR (125 MHz, acetone-d_6): δ 10.2 (C_{12}), 49.9 (C_{13}), 53.7 (C_{14}), 69.4 (C_{11}), 88.3 (η^6-C_6H_6), 121.8 (C_9), 124.2 (C_6), 125.6 (C_5), 127.0 (C_4), 128.4 (C_7), 132.4 (C_3), 134.2 (C_8), 136.6 (C_2), 137.2 (NCS), 151.1 (C_{10}), 164.2 (C_1). IR (Nujol): $\nu_{(CN)}$ 2107 cm^{-1} (shp, st), $\nu_{(CS)}$ 805 cm^{-1} (w). UV−vis (c = 1.8 × 10^{-4} M in CH_2Cl_2 at 25 °C): λ_{max}, nm (ϵ, L mol^{-1} cm^{-1}) 409 (1.8 × 10^3), 375 (1.4 × 10^3). CD, c = 1.8 × 10^{-4} M in CH_2Cl_2 at 25 °C: λ_{max}, nm ($[\theta]_\lambda$, deg cm^2 $dmol^{-1}$) 600 (0), 425 (+52326), 344 (−50009), 313 (−15873).

8b (X = NO_2): yield 0.164 g (77%). Anal. Calcd for $C_{20}H_{22}N_2O_2Ru$: C, 56.75; H, 5.20; N, 6.62. Found: C, 56.60; H, 5.14; N, 6.53. ^1H NMR (500 MHz, $CDCl_3$): δ 1.30 (d, $^3J(H_7H_{12})$ = 6.5 Hz, 3H, CH_3(12)), 2.48 (s, 3H, NCH_3(13)), 3.53 (s, 3H, NCH_3(14)), 4.03 (q, $^3J(H_7H_{12})$ = 6.5 Hz, 1H, H_7), 5.47 (s, 6H, η^6-C_6H_6), 7.17 (s, 1H, H_6), 7.29 (ddd, $^3J(H_4H_5)$ = 8.0 Hz, $^3J(H_3H_4)$ = 7.0 Hz, $^4J(H_2H_4)$ = 1.0 Hz, 1H, H_4), 7.39 (ddd, $^3J(H_2H_3)$ = 8.0 Hz, $^3J(H_3H_4)$ = 7.0 Hz, $^4J(H_3H_5)$ = 1.3 Hz, 1H, H_3), 7.66 (dd, $^3J(H_4H_5)$ = 8.0 Hz, $^4J(H_3H_5)$ = 1.3 Hz, 1H, H_5), 7.78 (dd, $^3J(H_2H_3)$ = 8.0 Hz, $^4J(H_2H_4)$ = 1.0 Hz, 1H, H_2), 8.63 (s, 1H, H_1). $^{13}C\{^1H\}$ NMR (125 MHz, $CDCl_3$): δ 9.81 (C_{12}), 50.9 (C_{13}), 52.1 (C_{14}), 67.9 (C_{11}), 88.9 (η^6-C_6H_6), 121.3 (C_9), 123.7 (C_6), 125.0 (C_5), 126.3 (C_4), 127.5 (C_7), 131.4 (C_3), 133.3 (C_8), 135.7 (C_2), 149.1 (C_{10}), 163.2 (C_1). IR (KBr): ν_a (NO_2) 1354 cm^{-1} (shp, st), ν_s (NO_2) 1299 cm^{-1} (shp, st), δ (ONO) 818 cm^{-1} (w), ρ_w (NO_2) 636 cm^{-1} (w). UV−vis (c = 1.8 × 10^{-4} M in CH_2Cl_2 at 25 °C): λ_{max}, nm (ϵ, L mol^{-1} cm^{-1}) 390 (1.5 × 10^3), 362 (1.4 × 10^3). CD, c = 1.8 × 10^{-4} M in CH_2Cl_2 at 25 °C: λ_{max}, nm ($[\theta]_\lambda$, deg cm^2 $dmol^{-1}$) 600 (0), 409 (+34160), 334 (−50852), 306 (−47991).

4. Synthesis and Characterization of the Ligand-Substituted Cationic Complexes {(η^6-C_6H_6)Ru[$C_{10}H_6CH$(Me)NMe_2](L)}$^+PF_6^-$. These ligand-substituted cationic complexes were all prepared by the same general method. This involved reaction of **2a,a′** with the appropriate ligand in the presence of $NaPF_6$ in a mixture of CH_2Cl_2 and EtOH (100%). For the CH_3CN complex **2a,a′** was reacted with CH_3CN, which was used as the solvent in the presence of $NaPF_6$. PDBP[19] and Ph_3P were recrystallized from hot EtOH (95%) under nitrogen before use, and allylisonitrile[17] was distilled under vacuum. All other ligands were reagent grade (Aldrich) and were used as received. All reactions were carried out under a dry dinitrogen atmosphere at ambient temperature. The following procedure for the preparation of **10c,c′** is representative.

10c,c′ (L = py). A mixture of **2a,a′** (0.174 g, 0.422 mmol), pyridine (0.68 mL, 0.84 mmol), $NaPF_6$ (0.143 g, 0.845 mmol)

in 2.5 mL of CH_2Cl_2, and 60 mL of absolute ethanol (mustard-yellow transparent solution) was stirred at ambient temperature for 16 h under a dry nitrogen atmosphere. The solvents were then removed on a rotary evaporator, and the residue (an orange-yellow powder) was washed with several small portions of a hexane/ether (1:1) mixture. The remaining yellow solid was dissolved in a minimum amount of CH_2Cl_2 and filtered through a short column of alumina, which had been packed with a mixture of hexane/ether (1:1), and eluted with CH_2Cl_2. This allowed us to remove NaCl, excess $NaPF_6$, some organic impurities, and elemental ruthenium. The transparent yellow eluate was collected, and the solvents were removed on a rotary evaporator. The remaining yellow solid was dried in vacuo to afford the product as a yellow powder; yield 0.33 g (75%). Anal. Calcd for $C_{25}H_{27}F_6N_2PRu$: C, 49.95; H, 4.49; N, 4.66. Found: C, 50.01; H, 4.52; N, 4.39. ^{1}H NMR (500 MHz, acetone-d_6): **10c** (major) δ 1.30 (d, $^3J(H_7H_{12}) = 6.5$ Hz, 3H, CH_3(12)), 2.70 (s, 3H, NCH_3(13)), 2.91 (qd, $^3J(H_7H_{12}) = 6.5$ Hz, $^4J(H_6H_7) = 1.0$ Hz, 1H, H_7), 3.45 (s, 3H, NCH_3(14)), 5.93 (s, 6H, η^6-C_6H_6), 7.13 (bs, 1H, py), 7.35 (d, $^4J(H_6H_7) = 1.0$ Hz, 1H, H_6), 7.39 (ddd, $^3J(H_4H_5) = 8.0$ Hz, $^3J(H_3H_4) = 7.0$ Hz, $^4J(H_2H_4) = 1.0$ Hz, 1H, H_4), 7.48 (ddd, $^3J(H_2H_3) = 8.0$ Hz, $^3J(H_3H_4) = 7.0$ Hz, $^4J(H_3H_5) = 1.0$ Hz, 1H, H_3), 7.60 (bs, 2H, py), 7.78 (dd, $^3J(H_4H_5) = 8.0$ Hz, $^4J(H_3H_5) = 1.0$ Hz, 1H, H_5), 7.92 (dd, $^3J(H_2H_3) = 8.0$ Hz, $^4J(H_2H_4) = 1.0$ Hz, 1H, H_2), 7.93 (tt, $^3J(HH) = 7.5$ Hz, $^4J(HH) = 1.5$ Hz, 1H, py H_4'), 9.06 (s, 1H, H_1), 9.93 (bs, 1H, py). That the pyridine $H_{o,m}$ resonances are broad unresolved multiplets while the pyridine H_4' resonance is sharp and well resolved indicates hindered rotation about the Ru−N(pyridine) bond: **10c′** (minor) δ 1.45 (d, $^3J(H_7H_{12}) = 6.5$ Hz, 3H, CH_3(12)), 2.78 (s, 3H, NCH_3(13)), 3.74 (s, 3H, NCH_3(14)), 4.35 (qd, $^3J(H_7H_{12}) = 6.5$ Hz, $^4J(H_6H_7) = 1.0$ Hz, 1H, H_7), 5.86 (s, 6H, η^6-C_6H_6), 7.13 (bs, 1H, py), 7.35 (d, $^4J(H_6H_7) = 1.0$ Hz, 1H, H_6), 7.39 (ddd, $^3J(H_4H_5) = 8.0$ Hz, $^3J(H_3H_4) = 7.0$ Hz, $^4J(H_2H_4) = 1.0$ Hz, 1H, H_4), 7.48 (ddd, $^3J(H_2H_3) = 8.0$ Hz, $^3J(H_3H_4) = 7.0$ Hz, $^4J(H_3H_5) = 1.0$ Hz, 1H, H_3), 7.60 (bs, 2H, py), 7.83 (dd, $^3J(H_4H_5) = 8.0$ Hz, $^4J(H_3H_5) = 1.0$ Hz, 1H, H_5), 7.85 (dd, $^3J(H_2H_3) = 8.0$ Hz, $^4J(H_2H_4) = 1.0$ Hz, 1H, H_2), 7.98 (tt, $^3J(HH) = 7.5$ Hz, $^4J(HH) = 1.5$ Hz, 1H, py H_4'), 8.60 (s, 1H, H_1), 8.67 (bs, 1H, py). The relative intensities of the two H_1 resonances (4.6:1) established the 64.2% de. ^{13}C{^{1}H} NMR (125 MHz, acetone-d_6): **10c** (major) δ 10.1 (C_{12}), 51.3 (C_{13}), 53.2 (C_{14}), 70.2 (C_{11}), 89.7 (η^6-C_6H_6), 123.2 (C_9), 125.2 (C_6), 126.4 (C_5), 126.9 (b, py), 127.4 (C_4), 128.7 (C_7), 132.9 (C_3), 134.9 (C_8), 137.1 (C_2), 139.8 (py, C_4'), 149.7 (C_{10}), 153.7 (b, py), 159.6 (b, py), 167.1 (C_1); **10c′** (minor) δ 11.0 (C_{12}), 43.4 (C_{13}), 56.4 (C_{14}), 77.3 (C_{11}), 89.4 (η^6-C_6H_6), 121.9 (C_9), 124.9 (C_6), 126.1 (C_5), 126.9 (b, py), 126.9 (C_4), 128.7 (C_7), 132.6 (C_3), 135.5 (C_8), 137.2 (C_2), 139.7 (py, C_4'), 151.2 (C_{10}), 153.7 (b, py), 159.6 (b, py), 172.8 (C_1). UV−vis ($c = 2.6 \times 10^{-4}$ M in CH_2Cl_2 at 25 °C): λ_{max}, nm (ϵ, L mol^{-1} cm^{-1}) 397 (2.7×10^3), 372 (2.6×10^3). CD, $c = 2.2 \times 10^{-4}$ M in CH_2Cl_2 at 25 °C: λ_{max}, nm ($[\theta]_\lambda$, deg cm^2 dmol^{-1}) 600 (0), 421 (+41863), 351 (−23191), 319 (−1551).

9c,c′ (L = CH_3CN): yield 0.286 g (70%). Because of the instability of this compound, satisfactory elemental analyses could not be obtained. ^{1}H NMR (500 MHz, acetone-d_6): **9c** (major) δ 1.42 (d, $^3J(H_7H_{12}) = 6.5$ Hz, 3H, CH_3(12)), 2.44 (s, 3H, CH_3CN), 2.82 (s, 3H, NCH_3(13)), 3.40 (s, 3H, NCH_3(14)), 3.97 (q, $^3J(H_7H_{12}) = 6.5$ Hz, 1H, H_7), 5.96 (s, 6H, η^6-C_6H_6), 7.35 (apparent t, $^3J(H_4H_5) = {}^3J(H_3H_4) = 8.0$ Hz, 1H, H_4), 7.35 (s, 1H, H_6), 7.42 (apparent t, $^3J(H_2H_3) = {}^3J(H_3H_4) = 8.0$ Hz, 1H, H_3), 7.75 (d, $^3J(H_4H_5) = 8.0$ Hz, 1H, H_5), 7.80 (d, $^3J(H_2H_3) = 8.0$ Hz, 1H, H_2), 8.73 (s, 1H, H_1); **9c′** (minor) δ 1.46 (d, $^3J(H_7H_{12}) = 6.5$ Hz, 3H, CH_3(12)), 2.02 (s, 3H, CH_3CN), 2.46 (s, 3H, NCH_3(13)), 3.58 (s, 3H, NCH_3(14)), 4.25 (q, $^3J(H_7H_{12}) = 6.5$ Hz, 1H, H_7), 5.88 (s, 6H, η^6-C_6H_6), 7.34 (apparent t, $^3J(H_4H_5) = {}^3J(H_3H_4) = 8.0$ Hz, 1H, H_4), 7.35 (s, 1H, H_6), 7.42 (apparent t, $^3J(H_2H_3) = {}^3J(H_3H_4) = 8.0$ Hz, 1H, H_3), 7.71 (d, $^3J(H_4H_5) = 8.0$ Hz, 1H, H_5), 7.80 (d, $^3J(H_2H_3) = 8.0$ Hz, 1H, H_2), 8.20 (s, 1H, H_1). The relative intensities of the two H_1 resonances (2.17:1) establish the 37% de. ^{13}C{^{1}H} NMR (125 MHz, acetone-d_6): **9c** (major) δ 4.1 (CH_3CN), 11.3 (C_{12}), 50.8 (C_{13}), 54.7 (C_{14}), 70.9 (C_{11}), 90.1 (η^6-C_6H_6), 122.4 (C_9), 124.8 (C_6), 126.0 (C_5), 127.1 (C_4), 127.5 (CH_3CN), 128.4 (C_7), 132.7 (C_3), 134.3 (C_8), 137.4 (C_2), 150.6 (C_{10}), 161.4 (C_1); **9c′** (minor) δ 3.8 (CH_3CN), 10.7 (C_{12}), 45.6 (C_{13}), 56.6 (C_{14}), 77.0 (C_{11}), 89.4 (η^6-C_6H_6), 122.0 (C_9), 124.6 (C_6), 126.0 (C_5), 126.7 (C_4), 127.4 (CH_3CN), 128.7 (C_7), 132.2 (C_3), 135.0 (C_8), 137.3 (C_2), 150.4 (C_{10}), 167.8 (C_1). IR (Nujol): $\nu_{(CN)}$ 2264 cm^{-1} (shp, st).

11c,c′ (L = 4-Me-py): yield 0.349 g (80%). Anal. Calcd for $C_{26}H_{29}F_6N_2PRu$: C, 50.75; H, 4.71; N, 4.55. Found: C, 50.70; H, 4.64; N, 4.61. ^{1}H NMR (500 MHz, acetone-d_6): **11c** (major) δ 1.29 (d, $^3J(H_7H_{12}) = 6.5$ Hz, 3H, CH_3(12)), 2.36 (s, 3H, NCH_3(13)), 2.69 (s, 3H, $pyCH_3$), 2.89 (qd, $^3J(H_7H_{12}) = 6.5$ Hz, $^4J(H_6H_7) = 1.0$ Hz, 1H, H_7), 3.42 (s, 3H, NCH_3(14)), 5.90 (s, 6H, η^6-C_6H_6), 6.95 (bs, 1H, py), 7.35 (d, $^4J(H_6H_7) = 1.0$ Hz, 1H, H_6), 7.38 (ddd, $^3J(H_4H_5) = 8.0$ Hz, $^3J(H_3H_4) = 6.5$ Hz, $^4J(H_2H_4) = 1.0$ Hz, 1H, H_4), 7.42 (bs, 2H, py), 7.48 (ddd, $^3J(H_2H_3) = 8.0$ Hz, $^3J(H_3H_4) = 6.5$ Hz, $^4J(H_3H_5) = 1.0$ Hz, 1H, H_3), 7.78 (dd, $^3J(H_4H_5) = 8.0$ Hz, $^4J(H_3H_5) = 1.0$ Hz, 1H, H_5), 7.91 (dd, $^3J(H_2H_3) = 8.0$ Hz, $^4J(H_2H_4) = 1.0$ Hz, 1H, H_2), 9.04 (s, 1H, H_1), 9.71. (bs, 1H, py); **11c′** (minor) δ 1.45 (d, $^3J(H_7H_{12}) = 6.5$ Hz, 3H, CH_3(12)), 2.31 (s, 3H, NCH_3(13)), 2.79 (s, 3H, $pyCH_3$), 3.72 (s, 3H, NCH_3(14)), 4.33 (qd, $^3J(H_7H_{12}) = 6.5$ Hz, $^4J(H_6H_7) = 1.0$ Hz, 1H, H_7), 5.83 (s, 6H, η^6-C_6H_6), 6.95 (bs, 1H, py), 7.35 (d, $^4J(H_6H_7) = 1.0$ Hz, 1H, H_6), 7.37 (ddd, $^3J(H_4H_5) = 8.0$ Hz, $^3J(H_3H_4) = 6.5$ Hz, $^4J(H_2H_4) = 1.0$ Hz, 1H, H_4), 7.42 (bs, 2H, py), 7.47 (ddd, $^3J(H_2H_3) = 8.0$ Hz, $^3J(H_3H_4) = 6.5$ Hz, $^4J(H_3H_5) = 1.0$ Hz, 1H, H_3), 7.81 (dd, $^3J(H_4H_5) = 8.0$ Hz, $^4J(H_3H_5) = 1.0$ Hz, 1H, H_5), 7.84 (dd, $^3J(H_2H_3) = 8.0$ Hz, $^4J(H_2H_4) = 1.0$ Hz, 1H, H_2), 8.43 (s, 1H, H_1), 8.57 (bs, 1H, py). As with the pyridine analogue, there is hindered rotation about the Ru−N(pyridine) bond. The relative intensities of the two H_1 resonances (4.5:1) establish the 63.6% de. ^{13}C{^{1}H} NMR (125 MHz, acetone-d_6): **11c** (major) δ 10.1 (C_{12}), 20.8 ($pyCH_3$), 51.2 (C_{13}), 53.2 (C_{14}), 70.2 (C_{11}), 89.6 (η^6-C_6H_6), 123.2 (C_9), 125.1 (C_6), 126.3 (C_5), 127.4 (C_4), 127.9 (b, py), 128.7 (C_7), 132.9 (C_3), 134.8 (C_8), 137.1 (C_2), 149.8 (pyC_4), 152.0 (C_{10}), 152.8 (b, py), 158.7 (b, py), 167.8 (C_1); **11c′** (minor) δ 11.0 (C_{12}), 20.8 ($pyCH_3$), 43.4 (C_{13}), 56.4 (C_{14}), 77.2 (C_{11}), 89.3 (η^6-C_6H_6), 121.8 (C_9), 124.8 (C_6), 126.1 (C_5), 127.2 (C_4), 127.9 (b, py), 128.7 (C_7), 132.6 (C_3), 135.4 (C_8), 137.1 (C_2), 149.8 (pyC_4), 151.3 (C_{10}), 152.8 (b, py), 158.7 (b, py), 173.0 (C_1). UV−vis ($c = 2.6 \times 10^{-4}$ M in CH_2Cl_2 at 25 °C): λ_{max}, nm (ϵ, L mol^{-1} cm^{-1}) 398 (2.2×10^3), 367 (2.0×10^3). CD, $c = 2.2 \times 10^{-4}$ M in CH_2Cl_2 at 25 °C: λ_{max}, nm ($[\theta]_\lambda$, deg cm^2 dmol^{-1}) 600 (0), 421 (+34289), 349 (−20229), 316 (−1320).

12c (L = $CNCH_2CH{=}CH_2$): yield 1.12 g (80%). Anal. Calcd for $C_{24}H_{27}F_6N_2PRu$: C, 48.92; H, 4.58; N, 4.75. Found: C, 48.73; H, 4.52; N, 4.69. ^{1}H NMR (500 MHz, acetone-d_6): δ 1.46 (d, $^3J(H_7H_{12}) = 6.5$ Hz, 3H, CH_3(12)), 2.70 (s, 3H, NCH_3(13)), 3.42 (s, 3H, NCH_3(14)), 4.04 (qd, $^3J(H_7H_{12}) = 6.5$ Hz, $^4J(H_6H_7) = 1.0$ Hz, 1H, H_7), 4.51 (m, $^2J(AB) = 17.0$ Hz, $^3J(H_aCH_2) = 4.5$ Hz, $^3J(H_bCH_2) = {}^3J(H_cCH_2) = 1.5$ Hz, 2H, CH_2), 5.07 (dt, $^3J(H_aH_b) = 17.0$ Hz, $^3J(H_bCH_2) = 1.5$ Hz, 1H, H_b), 5.08 (dt, $^3J(H_aH_c) = 10.5$ Hz, $^3J(H_cCH_2) = 1.5$ Hz, 1H, H_c), 5.82 (ddt, $^3J(H_aH_b) = 17.0$ Hz, $^3J(H_aH_c) = 10.5$ Hz, $^3J(H_aCH_2) = 4.5$ Hz, 1H, H_a), 6.31 (s, 6H, η^6-C_6H_6), 7.34 (ddd, $^3J(H_2H_3) = 8.0$ Hz, $^3J(H_3H_4) = 6.8$ Hz, $^4J(H_3H_5) = 1.0$ Hz, 1H, H_3), 7.40 (ddd, $^3J(H_4H_5) = 8.0$ Hz, $^3J(H_3H_4) = 6.8$ Hz, $^4J(H_2H_4) = 1.0$ Hz, 1H, H_4), 7.43 (d, $^4J(H_6H_7) = 1.0$ Hz, 1H, H_6), 7.71 (dd, $^3J(H_4H_5) = 8.0$ Hz, $^4J(H_3H_5) = 1.0$ Hz, 1H, H_5), 7.76 (dd, $^3J(H_2H_3) = 8.0$ Hz, $^4J(H_2H_4) = 1.0$ Hz, 1H, H_2), 8.35 (s, 1H, H_1). ^{13}C{^{1}H} NMR (125 MHz, acetone-d_6): δ 11.5 (C_{12}), 47.8 (CH_2), 51.9 (C_{13}), 57.9 (C_{14}), 74.3 (C_{11}), 96.1 (η^6-C_6H_6), 117.5 ($=CH_2$), 122.9 (C_9), 124.9 (C_5), 126.2 (C_6), 126.6 (C_7), 128.5 (C_4), 130.5 ($HC=$), 132.5 (C_3), 134.4 (C_8), 138.7 (C_2), 147.8 (CN), 152.2 (C_{10}), 155.4 (C_1). UV−vis ($c = 1.76 \times 10^{-4}$ M in CH_2Cl_2 at 25 °C): λ_{max}, nm (ϵ, L mol^{-1} cm^{-1}) 370 (2.0×10^3), 331 (5.6×10^3). CD, $c = 1.76 \times 10^{-4}$ M in CH_2Cl_2 at 25 °C: λ_{max}, nm ($[\theta]_\lambda$, deg cm^2 dmol^{-1})

600 (0), 390 (+17820), 330 (−171600), 291 (−478500), 269 (+22770). IR (KBr): $\nu_{(CN)}$ 2175 cm^{-1} (shp, st), $\nu_{(CC)}$ 1650 cm^{-1} (shp, w).

13c,c′ (L = Ph$_3$P). From the reaction of Ph_3P with **2a,a′** only one diastereomer was obtained, but two diastereomers were obtained from the reaction of the acetonitrile complex **9c,c′** in CH_2Cl_2/EtOH solution. The former reaction yielded 0.244 g (75%), while the later yielded 0.144 g (43%, after separation of the major diastereomer from the minor diastereomer by crystallization). Anal. Calcd for $C_{38}H_{37}F_6NP_2Ru$: C, 58.18; H, 4.72; N, 1.79. Found: C, 58.01; H, 4.65; N, 1.81. $^{31}P\{^1H\}$ NMR (202 MHz, acetone-d_6): **13c** (major) δ 30.79 (s, 1P, Ph_3P), −145.0 (sept, $^1J(PF) = 707.8$ Hz, 1P, PF_6^-); **13c′** (minor) δ 31.95 (s, 1P, Ph_3P), −145.0 (sept, $^1J(PF) = 707.8$ Hz, 1P, PF_6^-). ^1H NMR (500 MHz, acetone-d_6): **13c** (major) δ 0.96 (d, $^3J(H_7H_{12}) = 6.5$ Hz, 3H, CH_3(12)), 2.62 (s, 3H, NCH_3(13)), 2.81 (qd, $^3J(H_7H_{12}) = 6.5$ Hz, $^4J(H_6H_7) = 1.5$ Hz, 1H, H_7), 3.27 (s, 3H, NCH_3(14)), 5.95 (d, $J(PH) = 0.5$ Hz, 6H, η^6-C_6H_6), 6.99 (d, $^4J(H_6H_7) = 1.5$ Hz, 1H, H_6), 7.38 (m, 7H, $H_{m,}$ H_4), 7.52 (m, 10H, $H_{o,p}$, H_3), 7.71 (d, $^3J(H_4H_5) = 8.0$ Hz, 1H, H_5), 7.93 (d, $^3J(H_2H_3) = 8.0$ Hz, 1H, H_2), 8.75 (d, $^4J(PH) = 2.0$ Hz, 1H, H_1); **13c′** (minor) δ 1.39 (d, $^3J(H_7H_{12}) = 6.5$ Hz, 3H, CH_3(12)), 2.24 (s, 3H, NCH_3(13)), 3.42 (s, 3H, NCH_3(14)), 4.36 (qd, $^3J(H_7H_{12}) = 6.5$ Hz, $^4J(H_6H_7) = 1.0$ Hz, 1H, H_7), 5.94 (d, $J(PH) = 1.0$ Hz, 6H, η^6-C_6H_6), 7.40 (m, 11H, $H_{o,p}$, H_4, H_6), 7.54 (m, 7H, $H_{m,}$ H_3), 7.60 (d, $^3J(H_4H_5) = 8.0$ Hz, 1H, H_5), 7.90 (d, $^3J(H_2H_3) = 8.0$ Hz, 1H, H_2), 8.08 (s, 1H, H_1). The relative intensities of the phosphorus resonances and the two H_1 resonances (4:1) establish the 60% de. $^{13}C\{^1H\}$ NMR (125 MHz, acetone-d_6): **13c** (major) δ 9.6 (C_{12}), 53.1 (C_{13}), 57.8 (d, $^3J(PC) = 3.1$ Hz, C_{14}), 71.8 (d, $^3J(PC) = 1.1$ Hz, C_{11}), 95.3 (d, $J(PC) = 2.8$ Hz, η^6-C_6H_6), 123.8 (d, $^4J(PC) = 1.5$ Hz, C_9), 125.1 (C_6), 126.4 (C_5), 126.7 (C_4), 128.5 (C_7), 129.2 (d, $^3J(PC) = 9.7$ Hz, C_m), 131.7 (d, $^4J(PC) = 2.4$ Hz, C_p), 132.6 (d, $^4J(PC) = 1.3$ Hz, C_3), 134.2 (d, $^5J(PC) = 2.3$ Hz, C_8), 134.5 (d, $^1J(PC) = 43.9$ Hz, C_i), 135.3 (d, $^2J(PC) = 9.2$ Hz, C_o), 140.5 (d, $^3J(PC) = 5.8$ Hz, C_2), 150.8 (d, $^3J(PC) = 1.6$ Hz, C_{10}), 157.3 (d, $^2J(PC) = 22.9$ Hz, C_1). **13c′** (minor) δ 10.4 (C_{12}), 50.2 (C_{13}), 58.7 (C_{14}), 77.9 (C_{11}), 94.4 (d, $J(PC) = 2.6$ Hz, η^6-C_6H_6), 123.3 (C_9), 125.1 (C_6), 126.2 (C_5), 126.8 (C_4), 128.7 (C_7), 129.8 (d, $^3J(PC) = 7.5$ Hz, C_m), 131.8 (d, $^4J(PC) = 2.3$ Hz, C_p), 132.7 (C_3), 134.3 (C_8), 134.4 (d, $^1J(PC) = 43.9$ Hz, C_i), 135.3 (d, $^2J(PC) = 9.2$ Hz, C_o), 141.0 (d, $^3J(PC) = 7.8$ Hz, C_2), 151.0 (C_{10}), 160.3 (d, $^2J(PC) = 22.9$ Hz, C_1). UV−vis ($c = 4.4 \times 10^{-4}$ M in CH_2Cl_2 at 25 °C): λ_{max}, nm (ϵ, L mol^{-1} cm^{-1}) 403 (9.7×10^2), 372 (8.4×10^2). CD, $c = 4.4 \times 10^{-4}$ M and 4.4×10^{-5} in CH_2Cl_2 at 25 °C for 600−414 nm and 414−300 nm regions, respectively: λ_{max}, nm ($[\theta]_\lambda$, deg cm^2 $dmol^{-1}$) 600 (0), 436 (+10664), 334 (−59096), 316 (−6930).

14c,c′ (L = PDBP): yield 0.265 g (70%). Anal. Calcd for $C_{38}H_{35}F_6NP_2Ru$: C, 58.33; H, 4.47; N, 1.79. Found: C, 58.24; H, 4.40; N, 1.68.

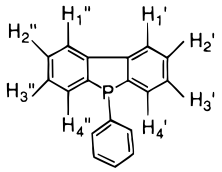

$^{31}P\{^1H\}$ NMR (202 MHz, $CDCl_3$): **14c** (major) δ 28.26 (s, 1P, PDBP), −144.98 (sept, $^1J(PF) = 707.4$ Hz, 1P, PF_6^-); **14c′** (minor) δ 28.17 (s, 1P, PDBP), −144.98 (sept, $^1J(PF) = 707.4$ Hz, 1P, PF_6^-). ^1H NMR (500 MHz, acetone-d_6): **14c** (major) δ 0.95 (d, $^3J(H_7H_{12}) = 6.5$ Hz, 3H, CH_3(12)), 2.45 (qd, $^3J(H_7H_{12}) = 6.5$ Hz, $^4J(H_6H_7) = 1.0$ Hz, 1H, H_7), 2.56 (s, 3H, NCH_3(13)), 2.63 (d, $^4J(PH) = 1.0$ Hz, 3H, NCH_3(14)), 5.92 (apparent t, $^3J(PH) = {}^3J(H_3'H_4') = 7.8$ Hz, 1H, H_4'), 6.11 (d, $J(PH) = 1.0$ Hz, 6H, η^6-C_6H_6), 6.61 (apparent tdd, $^3J(H_3'H_4') = {}^3J(H_2'H_3') = 7.8$ Hz, $^4J(PH) = 5.0$ Hz, $^4J(H_1'H_3') = 1.0$ Hz, 1H, H_3'), 7.23 (d, $^4J(H_6H_7) = 1.0$ Hz, 1H, H_6), 7.38 (apparent tt, $^3J(H_1'H_2') = {}^3J(H_2'H_3') = 7.8$ Hz, $^5J(PH) = {}^4J(H_2'H_4') = 1.5$ Hz, 1H, H_2'), 7.39 (m, 3H, $H_{m,p}$), 7.45 (ddd, $^3J(H_4H_5) = 8.0$ Hz, $^3J(H_3H_4) = 7.0$ Hz, $^4J(H_2H_4) = 1.0$ Hz, 1H, H_4), 7.58 (ddd, $^3J(H_2H_3) = 8.0$ Hz, $^3J(H_3H_4) = 7.0$ Hz, $^4J(H_3H_5) = 1.0$ Hz, 1H, H_3), 7.60 (m, 2H, H_o), 7.83 (m, 3H, H_2'', H_3'', H_5), 7.97 (apparent dt, $^3J(H_1'H_2') = 7.5$ Hz, $^4J(PH) = {}^4J(H_1'H_3') = 1.0$ Hz, 1H, H_1'), 8.01 (dd, $^3J(H_2H_3) = 8.0$ Hz, $^4J(H_2H_4) = 1.0$ Hz, 1H, H_2), 8.19 (apparent dt, $^3J(H_1''H_2'') = 7.0$ Hz, $^4J(PH) = {}^4J(H_1''H_3'') = 1.5$ Hz, 1H, H_1''), 8.67 (ddd, $^3J(H_3''H_4'') = 7.5$ Hz, $^4J(PH) = 5.0$ Hz, $^4J(H_2''H_4'') = 2.0$ Hz,1H, H_4''), 9.00 (d, $^3J(PH) = 2.0$ Hz, 1H, H_1); **14c′** (minor) δ 1.28 (d, $^3J(H_7H_{12}) = 6.5$ Hz, 3H, CH_3(12)), 2.89 (d, $^4J(PH) = 1.0$ Hz, 3H, NCH_3(13)), 3.10 (s, 3H, NCH_3(14)), 4.35 (qd, $^3J(H_7H_{12}) = 6.5$ Hz, $^4J(H_6H_7) = 1.0$ Hz, 1H, H_7), 5.92 (apparent t, $^3J(PH) = {}^3J(H_3'H_4') = 7.8$ Hz, 1H, H_4'), 6.07 (d, $J(PH) = 1.0$ Hz, 6H, η^6-C_6H_6), 6.77 (apparent tdd, $^3J(H_3'H_4') = {}^3J(H_2'H_3') = 7.8$ Hz, $^4J(PH) = 5.0$ Hz, $^4J(H_1'H_3') = 1.0$ Hz, 1H, H_3'), 7.25 (d, $^4J(H_6H_7) = 1.0$ Hz, 1H, H_6), 7.32 (m, 3H, $H_{m,p}$), 7.41 (ddd, $^3J(H_4H_5) = 8.0$ Hz, $^3J(H_3H_4) = 7.0$ Hz, $^4J(H_2H_4) = 1.0$ Hz, 1H, H_4), 7.50 (ddd, $^3J(H_2H_3) = 8.0$ Hz, $^3J(H_3H_4) = 7.0$ Hz, $^4J(H_3H_5) = 1.0$ Hz, 1H, H_3), 7.56 (m, 2H, H_o), 7.69 (m, 3H, H_2'', H_3'', H_5), 7.91 (apparent dt, $^3J(H_1'H_2') = 7.5$ Hz, $^4J(PH) = {}^4J(H_1'H_3') = 1.0$ Hz, 1H, H_1'), 7.96 (dd, $^3J(H_2H_3) = 8.0$ Hz, $^4J(H_2H_4) = 1.0$ Hz, 1H, H_2), 8.12 (apparent dt, $^3J(H_1''H_2'') = 7.0$ Hz, $^4J(PH) = {}^4J(H_1''H_3'') = 1.5$ Hz, 1H, H_1''), 8.71 (ddd, $^3J(H_3''H_4'') = 7.5$ Hz, $^4J(PH) = 5.0$ Hz, $^4J(H_2''H_4'') = 2.0$ Hz,1H, H_4''), 8.76 (s, 1H, H_1). The relative intensities of the phosphorus resonances and the two H_1 resonances (2.85:1) establishes the 48% de. $^{13}C\{^1H\}$ NMR (125 MHz, acetone-d_6): **14c** (major) δ 10.1 (C_{12}), 52.4 (C_{13}), 56.3 (d, $^3J(PC) = 3.3$ Hz, C_{14}), 74.1 (d, $^3J(PC) = 3.5$ Hz, C_{11}), 95.1 (d, $J(PC) = 2.8$ Hz, η^6-C_6H_6), 122.9 (C_9), 123.8 (d, $^3J(PC) = 5.7$ Hz, $C_{1,1'}$), 125.3 (C_6), 126.8 (C_5), 126.9 (C_4), 128.7 (C_7), 128.9 ($C_{2''}$), 129.0 ($C_{2'}$), 129.0 (d, $^3J(PC) = 10.2$ Hz, $C_{3,3'}$), 130.7 (d, $^3J(PC) = 9.9$ Hz, C_m), 130.8 (d, $^2J(PC) = 9.3$ Hz, $C_{4,4'}$), 131.4 (d, $^4J(PC) = 2.4$ Hz, C_8), 132.0 (d, $^2J(PC) = 9.9$ Hz, C_o), 132.1 (C_3), 133.8 (C_8), 135.4 (d, $^1J(PC) = 45.9$ Hz, C_i), 136.3 (d, $^1J(PC) = 49.3$ Hz, C_α), 137.0 (d, $^1J(PC) = 48.1$ Hz, C_α), 140.9 (d, $^3J(PC) = 3.1$ Hz, C_2), 142.3 (d, $^2J(PC) = 9.1$ Hz, C_β), 143.6 (d, $^2J(PC) = 8.8$ Hz, C_β), 150.5 (d, $^3J(PC) = 1.9$ Hz, C_{10}), 156.3 (d, $^2J(PC) = 24.4$ Hz, C_1). UV−vis ($c = 2.6 \times 10^{-4}$ M in CH_2Cl_2 at 25 °C): λ_{max}, nm (ϵ, L mol^{-1} cm^{-1}) 405 (1.0×10^3), 372 (8.0×10^2). CD, $c = 4.4 \times 10^{-4}$ M and 4.4×10^{-5} in CH_2Cl_2 at 25 °C for 600−427 nm and 427−300 nm regions, respectively: λ_{max}, nm ($[\theta]_\lambda$, deg cm^2 $dmol^{-1}$) 600 (0), 445 (+12407), 341 (−69197), 311 (+18982).

15c,c′ (L = DMPP): yield 0.335 g (65%). Anal. Calcd for $C_{32}H_{35}F_6NP_2Ru$: C, 54.11; H, 4.92; N, 1.97. Found: C, 54.00; H, 5.04; N, 2.01. $^{31}P\{^1H\}$ NMR (202 MHz, acetone-d_6): **15c** (major) δ 34.48 (s, 1P, DMPP), −145.0 (sept, $^1J(PF) = 707.4$ Hz, 1P, PF_6^-); **15c′** (minor) δ 42.72 (s, 1P, DMPP), −145.0 (sept, $^1J(PF) = 707.4$ Hz, 1P, PF_6^-). ^1H NMR (500 MHz, acetone-d_6): **15c** (major) δ 1.33 (d, $^3J(H_7H_{12}) = 6.5$ Hz, 3H, CH_3(12)), 1.96 (apparent t, $^4J(PH) = {}^4J(HH) = 1.5$ Hz, 3H, DMPP−CH_3), 1.99 (apparent t, $^4J(PH) = {}^4J(HH) = 1.5$ Hz, 3H, DMPP−CH_3), 2.67 (s, 3H, NCH_3(13)), 3.08 (d, $^4J(PH) = 1.0$ Hz, 3H, NCH_3(14)), 3.60 (qd, $^3J(H_7H_{12}) = 6.5$ Hz, $^4J(H_6H_7) = 1.0$ Hz, 1H, H_7), 5.96 (d, $J(PH) = 0.5$ Hz, 6H, η^6-C_6H_6), 6.20 (ddq, $^2J(PH) = 30.5$ Hz, $^4J(HH) = 2.0$ Hz, $^4J(HH) = 1.5$ Hz, 1H, H_α), 6.94 (ddq, $^2J(PH) = 34.0$ Hz, $^4J(HH) = 2.0$ Hz, $^4J(HH) = 1.5$ Hz, 1H, H_α), 7.25−7.40 (m, 7H, H_3, H_5, Ph), 7.37 (s, 1H, H_6), 7.46 (ddd, $^3J(H_4H_5) = 8.0$ Hz, $^3J(H_3H_4) = 7.0$ Hz, $^4J(H_2H_4) = 1.0$ Hz, 1H, H_4), 7.76 (dd, $^3J(H_2H_3) = 8.0$ Hz, $^4J(H_2H_4) = 1.0$ Hz, 1H, H_2), 8.31 (d, $^3J(PH) = 2.5$ Hz, 1H, H_1); **15c′** (minor) δ 1.45 (d, $^3J(H_7H_{12}) = 6.5$ Hz, 3H, CH_3(12)), 1.65 (apparent t, $^4J(PH) = {}^4J(HH) = 1.2$ Hz, 3H, DMPP−CH_3), 2.15 (d, $^4J(PH) = 4.5$ Hz, 3H, NCH_3(13)), 2.27 (apparent t, $^4J(PH) = {}^4J(HH) = 1.5$ Hz, 3H, DMPP−CH_3), 3.49 (s, 3H, NCH_3(14)), 4.44 (q, $^3J(H_7H_{12}) = 6.5$ Hz, 1H, H_7), 5.70 (ddq, $^2J(PH) = 34.0$ Hz, $^4J(HH) = 2.0$ Hz, $^4J(HH) = 1.2$ Hz, 1H, H_α), 6.18 (d, $J(PH) = 1.0$ Hz, 6H, η^6-C_6H_6), 6.82 (ddq, $^2J(PH) = 35.0$ Hz, $^4J(HH) = 2.0$ Hz, $^4J(HH) = 1.5$ Hz, 1H, H_α), 7.30 (ddd, $^3J(H_2H_3) = 8.0$ Hz, $^3J(H_3H_4) = 7.0$ Hz, $^4J(H_3H_5) = 1.0$ Hz, 1H, H_3), 7.36 (s,

1H, H_6), 7.39 (ddd, $^3J(H_4H_5)$ = 8.0 Hz, $^3J(H_3H_4)$ = 7.0 Hz, $^4J(H_2H_4)$ = 1.5 Hz, 1H, H_4), 7.48 (s, 1H, H_1), 7.49−7.55 (m, 3H, $H_{o,p}$), 7.56 (dd, $^3J(H_4H_5)$ = 8.0 Hz, $^4J(H_3H_5)$ = 1.0 Hz, 1H, H_5), 7.78 (dd, $^3J(H_2H_3)$ = 8.0 Hz, $^4J(H_2H_4)$ = 1.5 Hz, 1H, H_2), 7.90−7.96 (m, 2H, H_m). The relative intensities of the phosphorus resonances and the two H_1 resonances (1.5:1) establish the 20% de. $^{13}C\{^1H\}$ NMR (125 MHz, acetone-d_6): **15c** (major) δ 10.6 (C_{12}), 17.4 (d, $^3J(PC)$ = 5.8 Hz, DMPP−CH_3), 17.5 (d, $^3J(PC)$ = 5.8 Hz, DMPP−CH_3), 52.4 (C_{13}), 57.2 (d, $^3J(PC)$ = 4.0 Hz, C_{14}), 73.5 (C_{11}), 94.1 (d, $J(PC)$ = 2.8 Hz, η^6-C_6H_6), 123.0 (C_9), 124.9 (C_6), 126.3 (C_5), 126.6 (C_7), 126.9 (d, $^1J(PC)$ = 43.0 Hz, C_α), 127.5 (d, $^1J(PC)$ = 46.3 Hz, C_α), 128.6 (C_4), 129.2 (d, $^1J(PC)$ = 38.5 Hz, C_i), 129.6 (d, $^3J(PC)$ = 10.1 Hz, C_m), 131.2 (d, $^4J(PC)$ = 2.5 Hz, C_p), 132.3 (d, $^2J(PC)$ = 8.5 Hz, C_o), 132.6 (C_3), 134.4 (C_8), 139.7 (d, $^3J(PC)$ = 3.0 Hz, C_2), 151.1 (C_{10}), 153.1 (d, $^2J(PC)$ = 9.1 Hz, C_β), 153.2 (d, $^2J(PC)$ = 7.0 Hz, C_β), 157.1 (d, $^2J(PC)$ = 24.9 Hz, C_1); **15c′** (minor) δ 10.6 (C_{12}), 17.4 (d, $^3J(PC)$ = 5.0 Hz, DMPP−CH_3), 17.5 (d, $^3J(PC)$ = 5.5 Hz, DMPP−CH_3), 50.0 (d, $^3J(PC)$ = 8.3 Hz, C_{13}), 58.1 (C_{14}), 78.3 (C_{11}), 92.2 (d, $J(PC)$ = 2.6 Hz, η^6-C_6H_6), 122.3 (C_9), 124.6 (C_6), 126.0 (C_5), 126.3 (C_7), 127.9 (d, $^1J(PC)$ = 48.6 Hz, C_α), 128.7 (C_4), 129.8 (d, $^1J(PC)$ = 39.0 Hz, C_i), 130.2 (d, $^3J(PC)$ = 10.2 Hz, C_m), 130.5 (d, $^1J(PC)$ = 52.3 Hz, C_α), 132.1 (d, $^4J(PC)$ = 2.6 Hz, C_p), 132.5 (C_3), 133.7 (d, $^2J(PC)$ = 11.8 Hz, C_o), 134.3 (C_8), 138.0 (d, $^3J(PC)$ = 7.2 Hz, C_2), 150.1 (C_{10}), 153.1 (d, $^2J(PC)$ = 8.7 Hz, C_β), 154.7 (d, $^2J(PC)$ = 7.9 Hz, C_β), 159.9 (d, $^2J(PC)$ = 20.4 Hz, C_1). UV−vis ($c = 2.6 \times 10^{-4}$ M in CH_2Cl_2 at 25 °C): λ_{max}, nm (ϵ, L mol^{-1} cm^{-1}) 400 (9.0×10^2). CD, $c = 4.4 \times 10^{-5}$ M in CH_2Cl_2 at 25 °C: λ_{max}, nm $([\theta]_\lambda$, deg cm^2 dmol^{-1}) 600 (0), 380 (+24750), 332 (+6600).

16c,c′ (L = Et$_3$P): yield 0.363 g (78%). Anal. Calcd for $C_{26}H_{37}F_6NP_2Ru$: C, 48.77; H, 5.78; N, 2.19. Found: C, 48.59; H, 5.71; N, 2.04. $^{31}P\{^1H\}$ NMR (202 MHz, $CDCl_3$): **16c** (major) δ 16.60 (s, 1P, Et_3P), −145.0 (sept, $^1J(PF)$ = 714.0 Hz, 1P, PF_6^-); **16c′** (minor) δ 19.05 (s, 1P, Et_3P), −145.0 (sept, $^1J(PF)$ = 714.0 Hz, 1P, PF_6^-). ^1H NMR (500 MHz, acetone-d_6): **16c** (major) δ 0.98 (dt, $^3J(PH)$ = 15.0 Hz, $^3J(HH)$ = 7.5 Hz, 9H, PCH_2CH_3), 1.46 (d, $^3J(H_7H_{12})$ = 6.5 Hz, 3H, CH_3(12)), 1.92 ($ABMX_3$, $^2J(AB)$ = 15.5 Hz, $^2J(PH)$ = $^3J(HH)$ = 7.5 Hz, 3H, PCH_2), 1.94 ($ABMX_3$, $^2J(AB)$ = 15.5 Hz, $^2J(PH)$ = $^3J(HH)$ = 7.5 Hz, 3H, PCH_2), 2.67 (s, 3H, NCH_3(13)), 3.26 (s, 3H, NCH_3(14)), 3.74 (qd, $^3J(H_7H_{12})$ = 6.5 Hz, $^4J(H_6H_7)$ = 1.2 Hz, 1H, H_7), 6.11 (d, $J(PH)$ = 0.5 Hz, 6H, η^6-C_6H_6), 7.32 (ddd, $^3J(H_4H_5)$ = 8.0 Hz, $^3J(H_3H_4)$ = 7.0 Hz, $^4J(H_2H_4)$ = 1.0 Hz, 1H, H_4), 7.40 (d, $^4J(H_6H_7)$ = 1.2 Hz, 1H, H_6), 7.40 (ddd, $^3J(H_2H_3)$ = 8.0 Hz, $^3J(H_3H_4)$ = 7.0 Hz, $^4J(H_3H_5)$ = 1.2 Hz, 1H, H_3), 7.71 (dd, $^3J(H_4H_5)$ = 8.0 Hz, $^4J(H_3H_5)$ = 1.2 Hz, 1H, H_5), 7.76 (dd, $^3J(H_2H_3)$ = 8.0 Hz, $^4J(H_2H_4)$ = 1.0 Hz, 1H, H_2), 8.41 (d, $^3J(PH)$ = 2.5 Hz, 1H, H_1); **16c′** (minor) δ 1.07 (dt, $^3J(PH)$ = 15.0 Hz, $^3J(HH)$ = 7.5 Hz, 9H, PCH_2CH_3), 1.48 (d, $^3J(H_7H_{12})$ = 6.8 Hz, 3H, CH_3(12)), 1.91 ($ABMX_3$, $^2J(AB)$ = 15.5 Hz, $^2J(PH)$ = $^3J(HH)$ = 7.5 Hz, 3H, PCH_2), 1.95 ($ABMX_3$, $^2J(AB)$ = 15.5 Hz, $^2J(PH)$ = $^3J(HH)$ = 7.5 Hz, 3H, PCH_2), 2.24 (d, $^4J(PH)$ = 3.0 Hz, 3H, NCH_3(13)), 3.42 (s, 3H, NCH_3(14)), 4.39 (qd, $^3J(H_7H_{12})$ = 6.8 Hz, $^4J(H_6H_7)$ = 1.2 Hz, 1H, H_7), 6.01 (d, $J(PH)$ = 1.0 Hz, 6H, η^6-C_6H_6), 7.31 (ddd, $^3J(H_4H_5)$ = 8.0 Hz, $^3J(H_3H_4)$ = 6.8 Hz, $^4J(H_2H_4)$ = 1.0 Hz, 1H, H_4), 7.40 (ddd, $^3J(H_2H_3)$ = 8.0 Hz, $^3J(H_3H_4)$ = 6.8 Hz, $^4J(H_3H_5)$ = 1.2 Hz, 1H, H_3), 7.42 (d, $^4J(H_6H_7)$ = 1.2 Hz, 1H, H_6), 7.64 (dd, $^3J(H_4H_5)$ = 8.0 Hz, $^4J(H_3H_5)$ = 1.2 Hz, 1H, H_5), 7.79 (dd, $^3J(H_2H_3)$ = 8.0 Hz, $^4J(H_2H_4)$ = 1.0 Hz, 1H, H_2), 8.00 (s, 1H, H_1).The relative intensities of the phosphorus resonances and the two H_1 resonances (1.4:1) establish the 16% de. $^{13}C\{^1H\}$ NMR (125 MHz, acetone-d_6): **16c** (major) δ 8.3 (d, $^2J(PC)$ = 2.3 Hz, PCH_2CH_3), 10.5 (C_{12}), 20.6 (d, $^1J(PC)$ = 27.0 Hz, PCH_2), 52.9 (C_{13}), 57.3 (d, $^3J(PC)$ = 2.6 Hz, C_{14}), 72.9 (C_{11}), 93.4 (d, $J(PC)$ = 2.6 Hz, η^6-C_6H_6), 123.1 (C_9), 124.6 (C_6), 126.3 (C_5), 126.4 (C_7), 128.6 (C_4), 132.4 (C_3), 134.3 (C_8), 139.8 (d, $^3J(PC)$ = 2.6 Hz, C_2), 151.1 (C_{10}), 158.4 (d, $^2J(PC)$ = 23.5 Hz, C_1); **16c′** (minor) δ 8.9 (d, $^2J(PC)$ = 2.3 Hz, PCH_2CH_3), 10.6 (C_{12}), 20.6 (d, $^1J(PC)$ = 26.6 Hz, PCH_2), 49.7 (d, $^3J(PC)$ = 4.8 Hz, C_{13}), 58.3 (C_{14}), 77.7 (C_{11}), 92.5 (d, $J(PC)$ = 2.5 Hz, η^6-C_6H_6), 122.6 (d, $^4J(PC)$ = 1.0 Hz, C_9), 124.7 (C_6), 126.2 (C_5), 126.3 (C_7), 128.6 (C_4), 132.4 (C_3), 134.2 (C_8), 140.0 (d, $^3J(PC)$ = 5.4 Hz, C_2), 150.8 (C_{10}), 161.1 (d, $^2J(PC)$ = 19.6 Hz, C_1). UV−vis ($c = 4.0 \times 10^{-4}$ M in CH_2Cl_2 at 25 °C): λ_{max}, nm (ϵ, L mol^{-1} cm^{-1}) 378 (6.0×10^2), 335 (2.0×10^3), 331 (1.9×10^3), 320 (2.4×10^3), 316 (2.3×10^3). CD, $c = 4.0 \times 10^{-4}$ M in CH_2Cl_2 at 25 °C: λ_{max}, nm $([\theta]_\lambda$, deg cm^2 dmol^{-1}) 600 (0), 426 (+11748), 365 (+17837), 332 (−9135).

5. X-ray Data Collection and Processing. The crystal data and details of data collection are given in Table 1. Table 2 lists the color, habit, size, and the solvent mixture from which each of the crystals was obtained.

A suitable crystal of each compound was mounted on a glass fiber and placed on a Siemens P4 diffractometer. Intensity data were taken in the ω mode with graphite-monochromated Mo Kα radiation (λ = 0.710 73 Å). Three check reflections, monitored every 100 reflections, showed random (<2%) variation during the data collection. The data were corrected for Lorentz, and polarization effects and absorption (using an empirical model derived from azimuthal data collections). Scattering factors and corrections for anomalous dispersion were taken from a standard source.[25] Calculations were performed with the Siemens SHELXTL Plus (version 5.03) software package on a PC. The structures were solved by direct methods. Anisotropic thermal parameters were assigned to non-hydrogen atoms where appropriate. The solvent molecules for **11c**, **13c**, and **14c** were refined isotropically. Hydrogen atoms were refined at calculated positions with a riding model in which the C−H vector was fixed at 0.96 Å. The data were refined by the method of full-matrix least-squares on F^2. Final cycles of refinement gave the $R(F)$ and $R_w(F)$ values presented in Table 1, where $\omega^{-1} = \sigma^2F + 0.001F^2$. Absolute configurations were determined by refinements of the Flack parameter.[26] The known absolute configuration at the benzylic carbon of the starting mercury complex[5] and hence of **2a** also served as an internal reference in verifying the absolute configuration at the Ru(II) center in each of the ligand substitution products.

Acknowledgment. We thank Professor David A. Lightner for his generous permission to use the Jasco spectropolarimeter and Dr. Stephan Boidjiev for helpful discussions on CD techniques and spectra. This research was supported by an award from the Research Corporation, for which we are grateful. We are grateful to Johnson Matthey Aesar/Alfa for a generous loan of $RuCl_3 \cdot 3H_2O$, and to the National Science Foundation (Grant No. CHE-9214294) for funds to purchase the 500 MHz NMR spectrometer.

Supporting Information Available: For **2a, 3b, 4b, 5b, 6b, 7b, 8b, 10c, 11c, 12c, 13c, 14c, 15c′**, and **16c′**, tables of X-ray crystallographic data including crystallographic data, atomic coordinates, hydrogen atom coordinates, anisotropic thermal parameters, and interatomic distances and angles. This material is available free of charge via the Internet at http://pubs.acs.org.

OM980895C

(25) *International Tables for X-ray Crystallography*; D. Reidel Publishing Co.: Boston, MA, 1992; Vol. C.
(26) Flack, H. D. *Acta Crystallogr.* **1983**, *A39*, 876.